Intl. Journal of Robotics Research

Decoupled Nonlinear Adaptive Control of Position and Stiffness for Pneumatic Soft Robots

Maja Trumić[1,2], Kosta Jovanović[2], Adriano Fagiolini[1]

Abstract

This paper addresses the problem of simultaneous and robust closed-loop control of joint stiffness and position, for a class of antagonistically actuated pneumatic soft robots with rigid links and compliant joints. By introducing a first-order dynamic equation for the stiffness variable and using the additional control degree of freedom, embedded in the null space of the pneumatic actuator matrix, an innovative control approach is introduced comprising an adaptive compensator and a dynamic decoupler. The proposed solution builds upon existing adaptive control theory and provides a technique for closing the loop on joint stiffness in pneumatic variable stiffness actuators. Under a very mild assumption involving the inertia and actuator matrices, the solution is able to cope with uncertainties of the model and, when the desired stiffness is constant or slowly-varying, also of the pneumatic actuator. Position and stiffness decoupling is achieved by the introduction of a first-order differential equation for an internal state variable of the controller, which takes into account the time derivative of pressure in the stiffness dynamics. A formal proof of the stability of the position and stiffness tracking errors is provided. An appealing property of the approach is that it does not require higher derivatives of position or any derivatives of stiffness. The solution is validated with respect to several use-cases, first in simulation and then via a real pneumatic soft robot with McKibben muscles. A comparison with respect to existing techniques reveals a more robust position and stiffness tracking skill.

Keywords

Soft robots, variable stiffness actuators, pneumatic actuators, antagonistic drives, physical human-robot interaction, null-space, adaptive control.

Introduction

The aspiration to achieve or even surpass human dexterity and promptness in performing motion and manipulation tasks has fostered the development of robots with embedded flexibility in last decades. Contrary to previous practice, when robots' elasticity was sought to be suppressed, nowadays it is purposely introduced and encouraged in order to create a human-friendly, energy-optimized, and lightweight soft robots with the high force-to-weight ratio. Thanks to these properties, soft robots have shown promising aspects as far as it concerns the assistance and safe interaction with humans. Creating shared human-robot workplace would have positive social and economic influence (Ajoudani et al. (2018)), while human-robot collaboration would radically improve the health of manufacturing workers if robots would assist them in carrying heavy equipment (Cherubini et al. (2016)). Moreover, the idea of soft robot design has led to the development of effective prosthetic devices such as tendon-driven PISA/IIT SoftHand Pro-H (Piazza et al. (2017)), while there is still an ongoing research in developing energy-efficient autonomous mobile soft robots (Verrelst et al. (2005); Niiyama et al. (2007); Semini et al. (2011); Seok et al. (2015)).

Compliance of soft robots, with flexibility concentrated at joints, can be achieved by several different mechanisms (Vanderborght et al. (2013)). Among them, Variable Stiffness Actuators (VSA) seem to be most auspicious in typical applications (Grioli et al. (2015)), over-performing rigid robots regarding robustness and load-to-weight ratio (Bicchi and Tonietti (2002); Albu-Schäffer et al. (2007)).

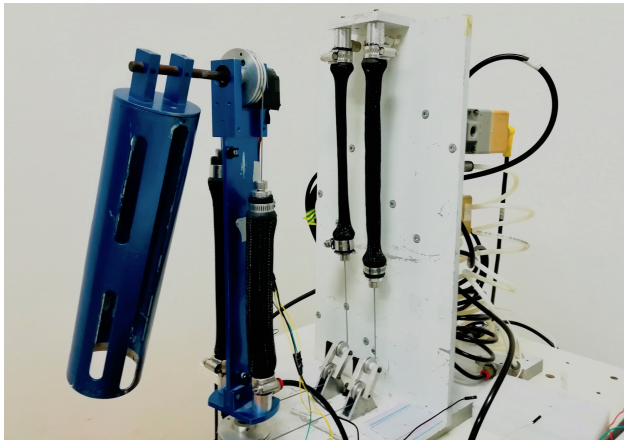

Figure 1. GioSte - Pneumatic soft robot arm designed and developed at the University of Pisa.

[1]Department of Engineering, University of Palermo, Italy
[2]School of Electrical Engineering, University of Belgrade, Serbia

Corresponding author:
Adriano Fagiolini, Department of Engineering, University of Palermo, Palermo, Italy.
Email: fagiolini@unipa.it

Their actuation can be either electrically, pneumatically or hydraulically powered. Even though most attention is nowadays drawn to the electrically powered VSA, pneumatic actuators still have benefits as for the higher power-to-weight ratio and simplicity of the mechanism (Caldwell et al. (1995); Van Ham et al. (2009)). The biologically inspired agonist-antagonistic setups of VSAs enable online compliance adaptation, which is of the utmost importance when robots operate in anthropic environments (Haddadin et al. (2009); Bicchi and Tonietti (2004)).

The compliance of a non-interactive robot is usually set in open loop, which means that the elastic characteristic of a soft robot has to be obtained in advance, either by using analytical calculation from the datasheet of the VSA as in the work of Angelini et al. (2018), or performing model identification as carried out by Lukić et al. (2016); Lukic et al. (2019). On the contrary, closed loop stiffness control has several benefits, as it provides full state feedback and information about the dynamical relation between actuation system and joints. Stiffness feedback approaches enable the soft robot manipulator to be reactive to external disturbances (Hogan (1985)), e.g. in the case when there is a contact between the environment and the robot. They are advantageous when the goal is to store energy (Garabini et al. (2011); Keppler et al. (2016)) or to perform task that requires delicate contact with the environment (Albu-Schaffer and Hirzinger (2002); Ott et al. (2008)). Furthermore, if decoupling position and stiffness control is obtained, soft robots are able to achieve high position accuracy, while in the meantime realize a range of possible joint stiffness.

Several approaches have been proposed for joint stiffness and position control such as static and dynamic feedback linearization approach (De Luca and Lucibello (1998); Palli et al. (2008); Potkonjak et al. (2011)), and backstepping control law (Petit et al. (2015)). All the above-mentioned approaches assume that the dynamic model is precisely known, which complicates their practical implementations. Model predictive control and sliding mode control (Best et al. (2016)), as well as nonlinear adaptive control of position and stiffness (Tonietti and Bicchi (2002)) have been applied on pneumatically driven variable stiffness actuators. In both cases, exact knowledge of model parameters is not a precondition. Since the stiffness is controlled in open loop, the solution of Tonietti and Bicchi (2002) can still be improved in order to achieve safer solutions for anthropic environments. Current results exposed by Della Santina et al. (2017) and Angelini et al. (2018) indicate the importance of compliance preserving and show, by means of learning algorithms, that this can be achieved by reducing the effect of the feedback action and, on the contrary, reinforcing the feedforward term.

The contributions of this paper lay on the foundation of the works by Tonietti and Bicchi (2002); Bicchi and Tonietti (2002), Spong (1989), and Della Santina et al. (2017); Keppler et al. (2018). Compared to the work by Tonietti and Bicchi (2002), a first extension stems in the fact that the robot's stiffness is controlled in closed-loop, which benefits to the overall system safety. A second appealing feature of the proposed method is the use of the control degrees of freedom, associated with the null-space of the actuator

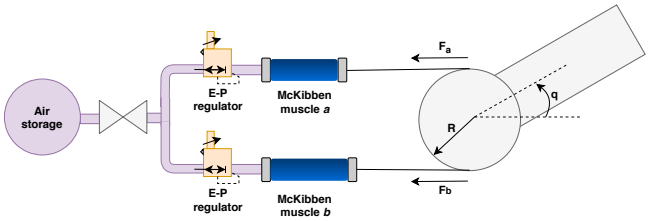

Figure 2. Depiction of a 1-DoF soft robotic arm actuated by a pair of McKibben artificial muscles in antagonistic configuration. Air pressure in the muscles is controlled by electro-pneumatic regulators and induces muscle contractions, thus allowing position and stiffness control of the robot's link.

matrix, to decouple the tracking of position commands from stiffness ones. The actuator matrix maps here the relation between muscle pressures and joint elastic torque. While the idea of using the null-space projections is not new in robotics — it has been applied to the Jacobian matrix of a redundant manipulator to achieve force (Khatib (1987)) and torque (Dietrich et al. (2015)) control — the presented approach enables the above-mentioned decoupling, without the necessity of higher order derivatives (cf. Palli et al. (2008); Keppler et al. (2018)), even when the system model is not perfectly known. The third contribution of this work is the experimental validation of the method on a real two-DoF soft robot arm with rigid links and flexible rotary joints, driven by pneumatically powered VSAs in an antagonistic setup. In the setup, artificial McKibben muscles are used as a flexible part of the pneumatic actuator system (Chou and Hannaford (1996); Gavrilović and Marić (1969)), behaving as springs with nonlinear characteristics due to the air compressibility.

Problem statement

Consider a soft robot with discrete points of elasticity coinciding with its n joints, provided with pneumatic actuation, which is used in applications requiring simultaneous regulation of joint position and stiffness. Having denoted with $q = (q_1, \cdots, q_n)^T$ and $S = (S_1, \cdots, S_n)^T$ the robot's position and stiffness vectors, respectively, in which q_i and S_i are the i-th joint angle and stiffness variables, a full model of the robot describing these vectors dynamics is required. As it is known, the position vector's dynamics is given by the differential equation:

$$B(q)\,\ddot{q} + C(q,\dot{q})\,\dot{q} + G(q) = \tau + \tau_{ext}\,, \qquad (1)$$

where $B(q) \in \mathbb{R}^{n\times n}$ is the inertia matrix, $C(q,\dot{q}) \in \mathbb{R}^n$ is the vector of Coriolis, centrifugal, and damping terms, $G(q) \in \mathbb{R}^n$ is the vector of gravity forces, $\tau = (\tau_1, \cdots, \tau_n)^T$ is the elastic torque vector, and $\tau_{ext} \in \mathbb{R}^n$ is the vector of external torque loads.

Moreover, consider the class of pneumatically driven robots with so-called McKibben artificial muscles in antagonistic configuration, where every joint i is actuated by a pair of muscles, a_i and b_i, attached to a pulley of radius R_i (Fig. 2). The i-th pair of muscles are responsible for providing the torque τ_i required for motion of the i-th joint, according to the static equation:

$$\tau_i = \tau_{i,a} - \tau_{i,b} = R_i F_{i,a}(q_i) - R_i F_{i,b}(q_i)\,,$$

where $F_{i,a}$ and $F_{i,b}$ are the elastic (tension) forces applied by the two muscles. The two forces of the pair of muscles depend on their internal pressures, $p_{i,a}$ and $p_{i,b}$. As in the work of Tonietti and Bicchi (2002), it can be assumed that the relations between elastic forces and pressures are expressed in the form

$$F_{i,a}(q_i) = K^g_{i,a}\,\phi_{i,a}(q_i)\,p_{i,a}\,,$$
$$F_{i,b}(q_i) = K^g_{i,b}\,\phi_{i,b}(q_i)\,p_{i,b}\,,$$

where $K^g_{i,a}$ and $K^g_{i,b}$ are construction-dependent muscle parameters, and $\phi_{i,a}(q_i)$ and $\phi_{i,b}(q_i)$ are the elongations of the muscles, given by the relations

$$\begin{aligned}\phi_{i,a}(q_i) &= (l_{i,a,n} - q_i R_i)^2 - l^2_{i,a,m}\,,\\ \phi_{i,b}(q_i) &= (l_{i,b,n} + q_i R_i)^2 - l^2_{i,b,m}\,,\end{aligned}$$

where $l_{i,a,n}$ and $l_{i,b,n}$ are the muscles' nominal lengths and $l_{i,a,m}$ and $l_{i,b,m}$ their minimum ones. To achieve a more compact form, let us assume for simplicity that each antagonistic pair of muscles have identical construction constants, i.e. $K^g_{i,a} = K^g_{i,b} = K^g_i$, and let us define the constants $K_i = K^g_i R_i$. Denoting then the diagonal construction-dependent constant matrix $K = \mathrm{diag}(K_i)$, the muscle elongation matrix $\Phi \in \mathbb{R}^{n\times 2n}$

$$\Phi(q) = \begin{pmatrix} \phi_{1,a}(q_1) & -\phi_{1,b}(q_1) & \dots & 0 & 0 \\ 0 & 0 & \ddots & \vdots & \vdots \\ 0 & 0 & \dots & \phi_{n,a}(q_n) & -\phi_{n,b}(q_n) \end{pmatrix},$$

and the pressure vector $p \in \mathbb{R}^{2n\times n}$ as

$$p = (p_{1,a}, p_{1,b}, p_{2,a}, p_{2,b}, \cdots, p_{n,a}, p_{n,b})^T\,,$$

the generalized elastic torque vector τ can be written as

$$\tau = K\,\Phi(q)\,p\,. \tag{2}$$

Eq 1 and 2 describe the dynamics of the joint position vector, under the actuation of the input pressure vector p.

Moving on now to the i-th joint's stiffness, by assuming that its pressure does not depend on its position, the stiffness itself can be obtained from its definition:

$$\begin{aligned} S_i &= -\frac{\partial \tau_i}{\partial q_i} = -K_i\left(\frac{\partial \phi_{i,a}}{\partial q_i}(q_i)\,p_{i,a} - \frac{\partial \phi_{i,b}}{\partial q_i}(q_i)\,p_{i,b}\right) = \\ &= -K_i\left(\phi_{q,i,a}(q_i)\,p_{i,a} - \phi_{q,i,b}(q_i)\,p_{i,b}\right)\,. \end{aligned}$$

Defining a matrix $\Phi_q(q)$ as

$$\begin{pmatrix} \phi_{q,1,a}(q_1) & -\phi_{q,1,b}(q_1) & \dots & 0 & 0 \\ 0 & 0 & \ddots & \vdots & \vdots \\ 0 & 0 & \dots & \phi_{q,n,a}(q_n) & -\phi_{q,n,b}(q_n) \end{pmatrix},$$

the stiffness vector can be written more concisely as

$$S = -K\,\Phi_q(q)\,p\,. \tag{3}$$

In order to obtain closed-loop control of the robot's stiffness S, a dynamic model for this variable is also needed. Inspired by the approach of De Luca and Lucibello (1998), this can be obtained by considering the first time derivative of S as in the following:

$$\dot{S} = -K\,\dot{\Phi}_q(q)\,p - K\,\Phi_q(q)\,\dot{p}\,. \tag{4}$$

Therefore, a full model of a soft-robot with pneumatic muscles can be obtained from Eq. 1, 2, 4, and thus written as

$$\begin{aligned} B(q)\,\ddot{q} + C(q,\dot{q})\,\dot{q} + G(q) &= K\,\Phi(q)\,p - \tau_{ext}\,,\\ \dot{S} &= -K\dot{\Phi}_q(q)\,p - K\Phi_q(q)\,\dot{p}\,, \end{aligned} \tag{5}$$

We will assume in the following that no interaction with the environment occurs, i.e. the external torque load is identically null ($\tau_{ext} = 0$ for all t), and that each pressure regulator is sufficiently fast to instantaneously control the corresponding pressure variable.

Within this setting, we are interested in solving the following:

Problem 1. Adaptive Decoupled Control. *Given a pneumatically driven soft robot as in Eq. 5, with joint position and stiffness vectors given by q and S, respectively, find a suitable control law for the input pressure p ensuring:*

- *decoupled closed-loop control of position and stiffness;*
- *robust asymptotic tracking with a complete lack of knowledge of inertial and geometric parameters;*
- *robust asymptotic tracking with a complete lack of knowledge of the construction-dependent parameters of the actuation model;*
- *practical implementability via the use of lower order derivatives of joint position and of stiffness estimates.*

The problem accounts for the possibility of simultaneously controlling position and stiffness, in an accurate way, by decoupling their commands. It also demands the avoidance of the use of joint acceleration and jerk and of stiffness time derivatives.

It is finally worth remarking that, since stiffness is not a measurable quantity, we must rely on either a dynamic stiffness estimator, such as the one proposed by Grioli and Bicchi (2010), or indirect model-based numerical computation, depending on other measurable quantities. The first type of solution needs no information about the system model, but it can be used only when the link is moving, while the second category is model-based, but it applies also when the link is at steady state. To this respect, the premise of stiffness depending on measurable state variables and control commands is common in practical implementations, for both electrically-driven VSAs (Migliore et al. (2007); Vanderborght et al. (2013); De Luca et al. (2009)) and pneumatically-driven ones (Vanderborght et al. (2008); Bicchi and Tonietti (2004); Colbrunn et al. (2001)). It can be further assumed, as we also do here, that no coupling between stiffnesses of different joints exists (Palli et al. (2008)). Following this approach, in our system, stiffness can be computed according to Eq 3, that is to the model derived in the work of Chou and Hannaford (1996).

Adaptive Decoupled Stiffness and Position Control

A novel nonlinear adaptive decoupled stiffness and position control is presented in this section. First, Proposition 1

briefly introduces the nonlinear adaptive control framework (Slotine and Li (1991)) underlying the proposed one. Afterwards, Proposition 2 provides the opportunity to assume uncertainty of both model and actuator parameters. This leads us to the main result of the paper presented in Theorem 1, where decoupling of position and stiffness control is achieved by an additional control degree-of-freedom, that exploits the actuator matrix's null-space. Finally, the stability of the proposed approach is analyzed and proved.

Given a robot with dynamical model of the form as in Eq. 1, it is known by e.g. Slotine and Li (1987) that the left-hand side expression of such a model can be conveniently factorized as the product of a *regressor* matrix $Y \in \mathbb{R}^{n\times\kappa}$ and a κ-dimensional vector $\pi \in \mathbb{R}^{\kappa}$ of uncertain parameters, i.e.

$$B(q)\,\ddot{q} + C(q,\dot{q})\,\dot{q} + G(q) = Y(q,\dot{q},\ddot{q})\,\pi\,. \tag{6}$$

It is important to note that the property also allows determining other regressor forms, as we do below, by linearly combining the matrices $B(q)$ and $C(q,\dot{q})$ and the vector $G(q)$ of the system's dynamics. By using this property, the following result can be proved (cf. the technique by Slotine and Li (1991)):

Proposition 1. *Given any desired joint trajectory $q_d : [0,\infty) \to \mathbb{R}^n$, with $q_d(t) \in \mathcal{C}^2$, a nonlinear adaptive controller ensuring asymptotic tracking of the joint evolution $q(t)$, for all initial parameter estimate $\hat{\pi}_0$, is described by the following dynamic system:*

$$\begin{aligned} \dot{\hat{\pi}} &= K_\pi\, Y^T(q,\dot{q},q_r,\dot{q}_r,\ddot{q}_r)\,\sigma\,, \\ \tau &= Y(q,\dot{q},q_r,\dot{q}_r,\ddot{q}_r)\,\hat{\pi} + K_d\,\sigma\,, \end{aligned} \tag{7}$$

where $\hat{\pi}$ and τ are the parameter estimate vector and the joint torque control, respectively, $\dot{q}_r = \dot{q}_d + \Lambda\,\tilde{q}$, $\sigma = \dot{\tilde{q}} + \Lambda\,\tilde{q}$, $\tilde{q} = q_d - q$, K_d and Λ are two positive definite matrices determining the tracking error convergence speed, and K_π is a positive definite matrix specifying the parameter adaptation rate.

Moreover, when the input control torque τ is applied to the robot through a flexible actuation system as in Eq. 2, whose model also includes separable uncertain parameters, the above result can be modified as suggested in the work by Tonietti and Bicchi (2002):

Proposition 2. *Given a flexible joint robotic system with pneumatic actuation model as in Eq. 2, with K a positive diagonal matrix, the nonlinear adaptive controller in Eq. 7 can be generalized as*

$$\begin{aligned} \dot{\hat{\Pi}} &= K_\pi\, Y_*^T(q,\dot{q},\dot{q}_r,\ddot{q}_r)\,\sigma\,, \\ p &= \Phi(q)^\dagger \left(Y_*(q,\dot{q},\dot{q}_r,\ddot{q}_r)\,\hat{\Pi} + K_d\,\sigma \right)\,, \end{aligned}$$

where $\hat{\Pi} \in \mathbb{R}^{\kappa_*}$ is a modified parameter vector also including the actuator uncertainties, and $\Phi(q)^\dagger \in \mathbb{R}^{2n\times n}$ is the pseudo-inverse of the known part of the actuator model.

Proof. Given the regressor form in Eq. 6 and the actuator model in Eq. 2, it holds

$$K\,\Phi(q)\,p = Y(q,\dot{q},\dot{q}_r,\ddot{q}_r)\,\pi\,.$$

Premultiplication by K^{-1} yields

$$\Phi(q)\,p = K^{-1}Y(q,\dot{q},\dot{q}_r,\ddot{q}_r)\,\pi = Y_*(q,\dot{q},\dot{q}_r,\ddot{q}_r)\,\Pi\,,$$

where Y_* is a suitable matrix allowing the factorization on the right of all unknown quantities into the modified parameter vector Π. The remainder of the proof straightforwardly follows. ■

Note that although $K = K_g R$ is immersed into the parameter vector Π, the joint pulley radius R must still be known, as it is part of the nonlinear expression of the actuator matrix.

When both desired stiffness and position signals have to be simultaneously tracked, a full model that also includes stiffness dynamics is more appropriate. Under the hypothesis that all system parameters are exactly known, this objective can be effectively achieved for flexible robots with electrically driven actuators, by using a dynamic feedback linearization approach of De Luca and Lucibello (1998). As it is known, the solution therein proposed obtains exact stiffness and position decoupling by exploiting information contained in higher-order derivatives of such variables.

On the contrary, when some system parameters are uncertain or even completely unknown, accurate and decoupled control can be achieved by endowing the controlled system with adaptivity capacity in different ways. One possible solution to achieve this is described in the following theorem, which leverages on the control degree of freedom obtained by projection to the actuator matrix's null-space. A depiction of the proposed nonlinear adaptive control is in Fig. 3.

Theorem 1. *Given a soft robot with dynamics as in Eq. 5, if matrix $K^{-1}B(q)$ is positive definite for all q, an adaptive and decoupling controller generating a pressure command signal $p(t)$, which allows simultaneous asymptotic tracking of any desired position and stiffness reference signals, $q_d : [0,\infty) \to \mathbb{R}^n$, with $q_d(t) \in \mathcal{C}^2$ and $S_d : [0,\infty) \to \mathbb{R}^n$, with $S_d(t) \in \mathcal{C}^1$, is described by the following system with dynamics given by*

$$\begin{aligned} \dot{\nu} \;=\; & \left(\Phi_q(q)\Phi(q)^\perp\right)^\dagger \Big(K_S(S - S_d) - K^{-1}\dot{S}_d \\ & - \Phi_q(q)\,\tfrac{d}{dt}\left(\Phi(q)^\dagger\tau_*\right) - \Phi_q(q)\Phi(q)^\dagger\tau_* + \\ & - \left(\Phi_q(q)\Phi(q)^\perp + \dot{\Phi}(q)^\perp\right)\nu \Big), \end{aligned} \tag{8}$$

$$\dot{\hat{\Pi}} = K_\pi\, Y_*^T(q,\dot{q},q_r,\dot{q}_r,\ddot{q}_r)\,\sigma\,, \tag{9}$$

and output signal given by

$$p = \Phi(q)^\dagger\tau_* + \Phi(q)^\perp\nu\,, \tag{10}$$

with

$$\tau_* = Y_*(q,\dot{q},\dot{q}_r,\ddot{q}_r)\,\hat{\Pi} + K_d\,\sigma\,, \tag{11}$$

where $\nu \in \mathbb{R}^n$ is an internal controller state, $\hat{\Pi} \in \mathbb{R}^{\kappa}$ is the estimated parameter vector, $\tau_* \in \mathbb{R}^n$ is a control signal directly affecting the applied torque, K_d, K_S, and K_π are positive definite matrices determining the convergence speed of the position tracking error, the stiffness tracking error, and the parameter estimation error, respectively, Y_* is a regressor matrix for the robot's position dynamics, $\Phi(q)^\dagger$ is the pseudo-inverse of $\Phi(q)$, $\Phi(q)^\perp$ is a matrix in the null

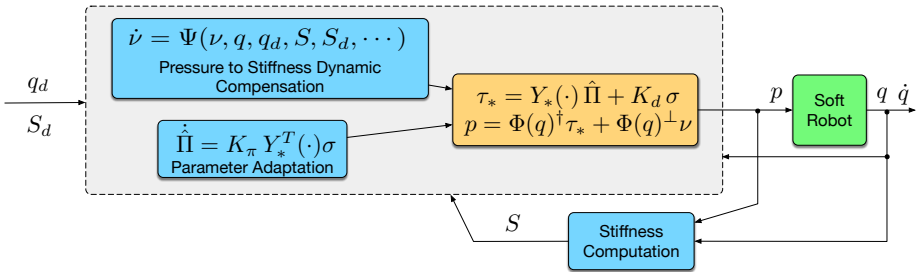

Figure 3. Depiction of the proposed decoupled nonlinear adaptive and decoupling control approach.

column-space of $\Phi(q)$*, and* $\Phi_q(q) = \frac{\partial \Phi}{\partial q}(q)$.
Note*: The theorem describes the state form of a dynamic controller whose internal variables,* ν *and* $\hat{\Pi}$*, are updated according to Eq. 8 and 9, and whose output* p*, can be algebraically computed by means of Eq. 10 and Eq. 11.*

Proof. The proof of the theorem is two stage. First, it can be proved that the full dynamic model of the robot can be rewritten in suitable regressor form, and thus that adaptive control laws for stiffness and position regulation can be found; then, it can be shown that such control laws can be converted to feasible pressure commands.

To begin with, from the property of Eq. 6, consider rewriting in regressor form the following expression, obtained from the first equation of the robot's dynamics:

$$\begin{aligned} &K^{-1}\left(B(q)\,\dot{\sigma} + \tfrac{1}{2}\dot{B}(q)\,\sigma\right) = \\ &= K^{-1}\left(B(q)\,(\ddot{q}_r - \ddot{q}) + \tfrac{1}{2}\dot{B}(q)\,\sigma\right) = \\ &= K^{-1}\left(B(q)\ddot{q}_r + C(\cdot)\,\dot{q} + G(q) + \tfrac{1}{2}\dot{B}(q)\sigma\right) - \Phi(q)\,p = \\ &= Y_*(q,\dot{q},\dot{q}_r,\ddot{q}_r)\,\Pi - \Phi(q)\,p\,, \end{aligned}$$

where Y_* is a suitable regressor matrix and Π is the corresponding parameter vector. Left-multiplying the second equation of the robot's dynamic model by K^{-1} yields

$$K^{-1}\dot{S} = -\dot{\Phi}_q(q)\,p - \Phi_q(q)\,\dot{p}\,.$$

Furthermore, having defined a new control torque vector τ_* and a *stiffness control* vector u_S as

$$\begin{aligned} \tau_* &= \Phi(q)\,p\,, \\ u_S &= -\dot{\Phi}_q(q)\,p - \Phi_q(q)\,\dot{p}\,, \end{aligned} \tag{12}$$

respectively, one obtains the following dynamic equations:

$$\begin{aligned} K^{-1}\left(B(q)\,\dot{\sigma} + \tfrac{1}{2}\dot{B}(q)\,\sigma\right) &= Y_*(q,\dot{q},\dot{q}_r,\ddot{q}_r)\,\Pi - \tau_*\,, \\ K^{-1}\dot{S} &= u_S\,. \end{aligned}$$

Then, under the hypothesis that $K^{-1}B(q)$ is positive definite for all q, one can adopt a similar approach as in Prop. 1 and find adaptive control laws for the new inputs, by also including, this time, a positive definite term depending on stiffness. To this aim, one can choose the candidate Lyapunov function

$$\begin{aligned} V &= \tfrac{1}{2}\sigma^T K^{-1} B(q)\sigma + \tfrac{1}{2}\tilde{\Pi}^T K_\pi^{-1}\tilde{\Pi} + \\ &\quad + \tfrac{1}{2}(S - S_d)^T\Gamma(q)(S - S_d)\,, \end{aligned}$$

where $\tilde{\Pi} = \Pi - \hat{\Pi}$, $\hat{\Pi}$ is the parameter estimate vector, and $\Gamma(q)$ is a positive definite matrix to be properly chosen.

The Lie derivative of V is

$$\begin{aligned} \dot{V} &= \dot{V}_1 + \tfrac{1}{2}(S - S_d)^T\dot{\Gamma}(q)(S - S_d) + \\ &\quad + (S - S_d)^T\Gamma(q)(\dot{S} - \dot{S}_d)\,, \end{aligned}$$

where

$$\begin{aligned} \dot{V}_1 &= \sigma^T K^{-1}\left(B(q)\,\dot{\sigma} + \tfrac{1}{2}\dot{B}(q)\,\sigma\right) - \tilde{\Pi}^T K_\pi^{-1}\dot{\hat{\Pi}} = \\ &= \sigma^T\left(Y_*(q,\dot{q},\dot{q}_r,\ddot{q}_r)\,\Pi - \tau_*\right) - \tilde{\Pi}^T K_\pi^{-1}\dot{\hat{\Pi}}\,. \end{aligned}$$

Choosing τ_* as in Eq. 11 leads to

$$\dot{V}_1 = -\sigma^T K_d\,\sigma + \sigma^T Y_*(q,\dot{q},\dot{q}_r,\ddot{q}_r)\,\tilde{\Pi} - \tilde{\Pi}^T K_\pi^{-1}\dot{\hat{\Pi}}\,.$$

The transposition of the second addend on the right-hand side of the above equation, which can be done since it is a scalar, allows factorizing the expression of $\dot{V}_1$ as

$$\dot{V}_1 = -\sigma^T K_d\,\sigma + \tilde{\Pi}^T\left(Y_*^T(q,\dot{q},\dot{q}_r,\ddot{q}_r)\,\sigma - K_\pi^{-1}\dot{\hat{\Pi}}\right)\,.$$

Adopting the update rule in Eq. 9 for $\dot{\hat{\Pi}}$ makes the second addend to vanish and finally allows reducing $\dot{V}$ to

$$\begin{aligned} \dot{V} &= -\sigma^T K_d\,\sigma + \tfrac{1}{2}(S - S_d)^T\dot{\Gamma}(q)(S - S_d) + \\ &\quad + (S - S_d)^T\Gamma(q)(\dot{S} - \dot{S}_d)\,. \end{aligned}$$

Moreover, the choice $\Gamma(q) = K^{-1}$ allows using the stiffness dynamics equation and is compliant with the positive definiteness of V. It also ensures $\dot{\Gamma}(q) = 0$, thereby making the time derivative $\dot{V}$ equal to

$$\begin{aligned} \dot{V} &= -\sigma^T K_d\,\sigma + (S - S_d)^T K^{-1}(\dot{S} - \dot{S}_d) = \\ &= -\sigma^T K_d\,\sigma + (S - S_d)^T u_S\,. \end{aligned}$$

Finally, by choosing the stiffness control input as

$$u_S = K^{-1}\dot{S}_d - K_s(S - S_d)\,, \tag{13}$$

one obtains

$$\dot{V} = -\sigma^T K_d\,\sigma - (S - S_d)^T K_S(S - S_d)\,.$$

which establishes the negative definiteness with respect to stiffness and position tracking errors. It is worth noticing that the parameter estimation convergence is not guaranteed, but their error remains bounded as it can be found from the study of the second time derivative and from Barbalat's Lemma.

Let us now move on to converting these controls into feasible pressure commands. To achieve this, first assume that the sought commanded pressure vector has the form

$$p = A_1(q)\,\tau_* + A_2(q)\,\nu\,,$$

where ν is another new control vector, and $A_1(q)$ and $A_2(q)$ are two position-dependent matrices to be conveniently chosen. From the first relation of Eq. 12, $\Phi(q)\,p = \tau_*$, one finds that it must be

$$\Phi(q)A_1(q)\,\tau_* + \Phi(q)A_2(q)\,\nu = \tau_*\,,$$

which can be satisfied if $\Phi(q)A_1(q) = I_n$ and $\Phi(q)A_2(q) = 0_n$, where I_n and 0_n are the identity and the zero matrix of dimension n. The first of the two conditions requires that $A_1(q) = \Phi(q)^T \left(\Phi(q)\,\Phi(q)^T\right)^{-1} = \Phi(q)^\dagger$, which is the pseudo-inverse of $\Phi(q)$, while the second one implies that $A_2(q) = \Phi(q)^\perp$, in which $\Phi(q)^\perp$ is any matrix in the column null-space of $\Phi(q)$. Therefore, the commanded pressure vector p can be determined as in the form

$$p = \Phi(q)^\dagger\,\tau_* + \Phi(q)^\perp\,\nu\,,$$

where ν is still to be determined. Moreover, after computing the time derivative of p, given by

$$\dot{p} = \frac{d}{dt}\left(\Phi(q)^\dagger\,\tau_*\right) + \dot{\Phi}(q)^\perp\,\nu + \Phi(q)^\perp\,\dot{\nu}\,,$$

one can write from Eq. 12 that it must hold

$$\begin{array}{rcl} u_S & = & -\dot{\Phi}_q(q)\,\Phi(q)^\dagger\tau_* - \dot{\Phi}_q(q)\Phi(q)^\perp\,\nu + \\ & & -\Phi_q(q)\left(\frac{d}{dt}\left(\Phi(q)^\dagger\,\tau_*\right) + \frac{d}{dt}\left(\Phi(q)^\perp\right)\,\nu + \right. \\ & & \left. +\Phi(q)^\perp\,\dot{\nu}\right)\,. \end{array}$$

Substituting in the above equation u_S with its expression from Eq. 13 and then solving it for $\dot{\nu}$ allows deriving the differential relation for the controller internal state ν described in Eq. 8. To this purpose, first multiply both sides of the equation by the pseudo-inverse of $\Phi_q(q)\,\Phi(q)^\perp$, as in

$$\begin{array}{c} \left(\Phi_q(q)\,\Phi(q)^\perp\right)^\dagger\left(K_s(S - S_d) - K^{-1}\dot{S}_d\right) = \\ = \left(\Phi_q(q)\,\Phi(q)^\perp\right)^\dagger\,\beta(q) + \dot{\nu}\,, \end{array}$$

with

$$\begin{array}{rcl} \beta(q) & = & \Phi_q(q)\,\frac{d}{dt}\left(\Phi(q)^\dagger\tau_*\right) + \dot{\Phi}_q(q)\Phi(q)^\dagger\tau_* + \\ & + & \left(\dot{\Phi}_q(q)\Phi(q)^\perp + \Phi_q(q)\,\frac{d}{dt}\left(\Phi(q)^\perp\right)\right)\nu\,, \end{array}$$

and then find the expression for $\dot{\nu}$. This concludes the search for a feasible and stabilizing pressure command vector and the theorem's proof. ■

Remark 1. *As it is known, while the adaptive control approach always allows tracking of position and stiffness references, even with inexact parameter knowledge, no guarantees can be provided about the convergence of such parameters (Slotine and Li (1991)). Indeed, once the position tracking error e has converged to zero, the variable σ becomes null, and the parameter adaptation stops (see Eq. 9).*

An explicit characterization of the achieved parameter estimation error is not simple and it is also reference-dependent. Once the position tracking error $\tilde{q}$ has converged, the following holds. By first writing the robot's dynamics in regressor form, on the left hand side, and applying the adaptive torque, on the right hand side, we have:

$$Y_*(\cdot)\,\Pi = \Phi(q)\left(\Phi(q)^\dagger Y_*(\cdot)\,\hat{\Pi} + \Phi(q)^\perp\nu\right)\,,$$

where the variable dependency of matrix Y_* has been omitted for space reasons. The orthogonality construction gives us independence on variable ν, which may in principle still evolve, thus leading to

$$Y_*(q,\dot{q},q_r,\dot{q}_r,\ddot{q}_r)\,\Pi = \Phi(q)\Phi(q)^\dagger Y_*(q,\dot{q},q_r,\dot{q}_r,\ddot{q}_r)\,\hat{\Pi}\,,$$

and consequently to

$$Y_*(q,\dot{q},q_r,\dot{q}_r,\ddot{q}_r)\left(\Pi - \hat{\Pi}\right) = 0\,,$$

which finally describes the surface on which the reached parameter estimation error must lie.

Apparently, when the desired stiffness S_d is time-varying, the controller depends also on the actuator parameters K. However, for applications in which S_d is slowly varying or piecewise constant, the following corollary to Theorem 1 provides a solution independent of the actuator parameters:

Corollary 1. *Under the hypotheses of Theorem 1, if the desired stiffness S_d is slowly varying or piecewise constant, the nonlinear decoupling and adaptive controller is described by Eq. 9, Eq. 10, Eq. 11 and*

$$\begin{array}{c} \dot{\nu} = \left(\Phi_q(q)\Phi(q)^\perp\right)^\dagger\left(K_S(S - S_d) - \Phi_q(q)\,\frac{d}{dt}\left(\Phi(q)^\dagger\tau_*\right) + \right. \\ \left. - \Phi_q(q)\Phi(q)^\dagger\tau_* - \left(\Phi_q(q)\Phi(q)^\perp + \dot{\Phi}(q)^\perp\right)\nu\right)\,, \end{array} \quad (14)$$

and thus it is independent of the actuator parameters K.

Proof. The proof straightforwardly follows from Theorem 1 by assuming that $\dot{S}_d = 0$. ■

Remark 2. *By a first interpretation of the formula in Eq. 10, describing the expression of the stabilizing pressure command, it can be understood that the two signals τ_* and ν independently control the robot's position and stiffness. While τ_* directly affects the applied torque, the differential form of ν takes into account for the term depending on $\dot{p}$, which is present in the stiffness dynamics.*

Remark 3. *It is also worth noticing that the time derivatives of the terms $\Phi^\dagger(q)\tau_*$ and $\Phi(q)^\perp$, involved in Eq. 8 of Th. 1 and in Eq. 14 of Corollary 1, can be either numerically computed or, more accurately computed in an analytical way by using the chain rule for differentiation. Indeed it holds:*

$$\frac{d}{dt}\left(\Phi^\dagger(q)\,\tau_*\right) = \Phi^\dagger_q(q)\,\dot{q}\,\tau_* + \Phi^\dagger(q)\frac{\partial\tau_*}{\partial q}\dot{q}\,.$$

The explicit calculation of the Jacobian of τ_* with respect to q are reported, for the reader convenience, in the experimental section. An analogous situation occurs when applying backstepping techniques.

Simulation Validation

This section presents a first step towards the validation of the proposed control approach. To this purpose, a two-degree-of-freedom, planar soft robot arm, actuated via antagonistic McKibben artificial muscles, has been considered. The aim of this section is to show how the proposed method effectively works, when exact knowledge of matrix $\Phi(q)$ is available. Under such ideal hypothesis, the only difference

Table 1. Definition and nominal values of the geometric and inertial parameters of the two-link soft robot. The real values of these parameters are assumed unknown.

Param.	Value	Unit	Description
m_1	0.44	kg	First link mass
m_2	0.35	kg	Second link mass
l_1	0.33	m	First link length
l_2	0.225	m	Second link length
I_1	0.004	kgm^2	First link inertia
I_2	0.0015	kgm^2	Second link inertia
g	9.81	m/s^2	Gravity constant

between the regressor form and the system's model in Eq. 6 is in the values of unknown parameters Π. The reported simulations show indeed how the controller continuously adjusts the estimated parameter vector $\hat{\Pi}$, as the robot's position q and stiffness S, are *exactly* steered to the desired values.

Having defined the robot's configuration vector as $q = (q_1, q_2)^T$, with q_1 the arm's shoulder angle and with q_2 its elbow angle, the robot's dynamic model can be written in the form of Eq. 5. As for the position's dynamic equation, the well-known expressions of the inertia and Coriolis matrices and of the gravity vector are standard* and can be found e.g. in the text by Siciliano and Khatib (2008). More precisely, referring to the system's parameters reported in Table 1, the inertia matrix is:

$$B(q) = \begin{pmatrix} B_{11}(q) & B_{12}(q) \\ B_{12}(q) & B_{22}(q) \end{pmatrix},$$

with

$$\begin{aligned} B_{11}(q) &= I_1 + m_1\left(\tfrac{l_1}{2}\right)^2 + I_2 + m_2 l_1^2, \\ &\quad + m_2\left(\tfrac{l_2}{2}\right)^2 + m_2 l_1 l_2 c_2, \\ B_{12}(q) &= I_2 + m_2\left(\tfrac{l_2}{2}\right)^2 + \tfrac{1}{2} m_2 l_1 l_2 c_2, \\ B_{22}(q) &= \tfrac{1}{2} m_2 l_2^2 + I_2, \end{aligned}$$

the matrix of Coriolis and centrifugal forces is

$$C(q,\dot{q}) = \begin{pmatrix} -\tfrac{1}{2} m_2 l_1 s_2 \dot{q}_2 & -\tfrac{1}{2} m_2 l_1 s_2 (\dot{q}_1 + \dot{q}_2) \\ \tfrac{1}{2} m_2 l_1 s_2 \dot{q}_1 & 0 \end{pmatrix},$$

and the vector containing gravitation components is

$$G(q) = \begin{pmatrix} (\tfrac{1}{2} m_1 l_1 + m_2 l_1) g s_1 + \tfrac{1}{2} m_2 l_2 g s_{12} \\ \tfrac{1}{2} m_2 l_2 g s_{12} \end{pmatrix}.$$

Furthermore, as for the right-hand-side of Eq. 5, under the assumption of equal muscle parameters, i.e. $K = \mathrm{diag}(K_1, K_1)$, having denoted with $p_{i,a}$ and $p_{i,b}$ the pressures of the two artificial muscles of the i-th link, for $i \in \{1, 2\}$, and also referring to Table 2, the actuator model is given by the formula:

$$\tau_* = \Phi(q)\, p, \tag{15}$$

where

$$\begin{aligned} \tau_* &= (\tau_{*,1}, \tau_{*,2})^T = \tau / K_1, \\ p &= (p_{1,a}, p_{1,b}, p_{2,a}, p_{2,b})^T, \end{aligned}$$

and

$$\Phi(q) = \begin{pmatrix} \phi_1(q) & -\phi_1(q) & 0 & 0 \\ 0 & 0 & \phi_2(q) & -\phi_2(q) \end{pmatrix},$$

Table 2. Definition of the actuator model's parameters.

Param.	Value	Unit	Description
R	0.03	m	Pulley radius
K_g	0.16	-	Actuator param.
l_{nom}	0.17	m	Nom. muscle length
l_{min}	0.14	m	Min. muscle length

with

$$\phi_i(q) = (l_{nom} - q_i R)^2 - l_{min}^2 .$$

Let us now move on to deriving the equations of the adaptive and decoupling controller of Th 1. First, it can be verified that the condition $K^{-1}B(q)$ to be positive definite is satisfied, thereby allowing the proposed control approach to be applied. The regressor matrix reads

$$Y_* = \begin{pmatrix} \ddot{q}_{1,r} & \ddot{q}_{2,r} & Y_{13} & s_1 & s_{12} \\ 0 & \ddot{q}_{1,r} + \ddot{q}_{2,r} & Y_{23} & 0 & s_{12} \end{pmatrix},$$

with

$$\begin{aligned} Y_{13} &= (2\ddot{q}_{1,r} + \ddot{q}_{2,r}) c_2 - \dot{q}_2 \left(\dot{q}_1 + \tfrac{1}{2}\dot{q}_2 + \dot{q}_{1,r} + \tfrac{1}{2}\dot{q}_{2,r}\right) s_2, \\ Y_{23} &= \ddot{q}_{1,r}\, c_2 + \left(\dot{q}_1^2 + \tfrac{1}{2}\dot{q}_1\dot{q}_2 - \tfrac{1}{2}\dot{q}_{1,r}\dot{q}_2\right) s_2, \end{aligned}$$

and the parameter vector is

$$\begin{aligned} \Pi &= (\Pi_1, \Pi_2, \Pi_3, \Pi_4, \Pi_5)^T \\ &= \tfrac{1}{K_1} \begin{pmatrix} I_1 + m_1\left(\tfrac{l_1}{2}\right)^2 + I_2 + m_2(\tfrac{l_2}{2})^2 + m_2 l_1^2 \\ I_2 + m_2\left(\tfrac{l_2}{2}\right)^2 \\ \tfrac{1}{2} m_2 l_1 l_2 \\ \left(\tfrac{1}{2} m_1 + m_2\right) l_1 g \\ \tfrac{1}{2} m_2 l_2 g \end{pmatrix}. \end{aligned}$$

The term $\Phi(q)^\dagger$ is the standard Moore-Penrose pseudo-inverse, which is omitted here for the sake of space, while the null-space projector $\Phi(q)^\perp$ is given by

$$\Phi(q)^\perp = \begin{pmatrix} \phi_1(q) & 0 \\ \phi_1(q) & 0 \\ 0 & \phi_2(q) \\ 0 & \phi_2(q) \end{pmatrix}.$$

The internal state of the controller is the two-dimensional vector $\nu = (\nu_1, \nu_2)^T$. Therefore, the sought adaptive and decoupling controller can be obtained by implementing the internal state vector dynamics for ν in Eq. 8 and the parameter adaptation law in Eq. 9 for $\hat{\Pi}$, and then computing the adaptive control τ_* as in Eq 11 and, finally, the output command pressure p as in Eq. 10.

In order to show the effectiveness of the proposed approach, results from a typical simulation run are presented in the following. In the simulation, the robot's artificial muscles are initially inflated, so as to reach a *preset* stiffness S of 2 Nm/rad. During this initial setup phase, no parameter adaptation is executed by setting the matrix gain K_π to zero, while as soon as the parameter adaptation is activated, K_π is set to 35. It is worth noticing that

*The following usual abbreviations have been used: $c_1 = \cos(q_1)$, $c_2 = \cos(q_2)$, $s_1 = \sin(q_1)$, $s_2 = \sin(q_2)$, $c_{12} = \cos(q_1 + q_2)$, and $s_{12} = \sin(q_1 + q_2)$.

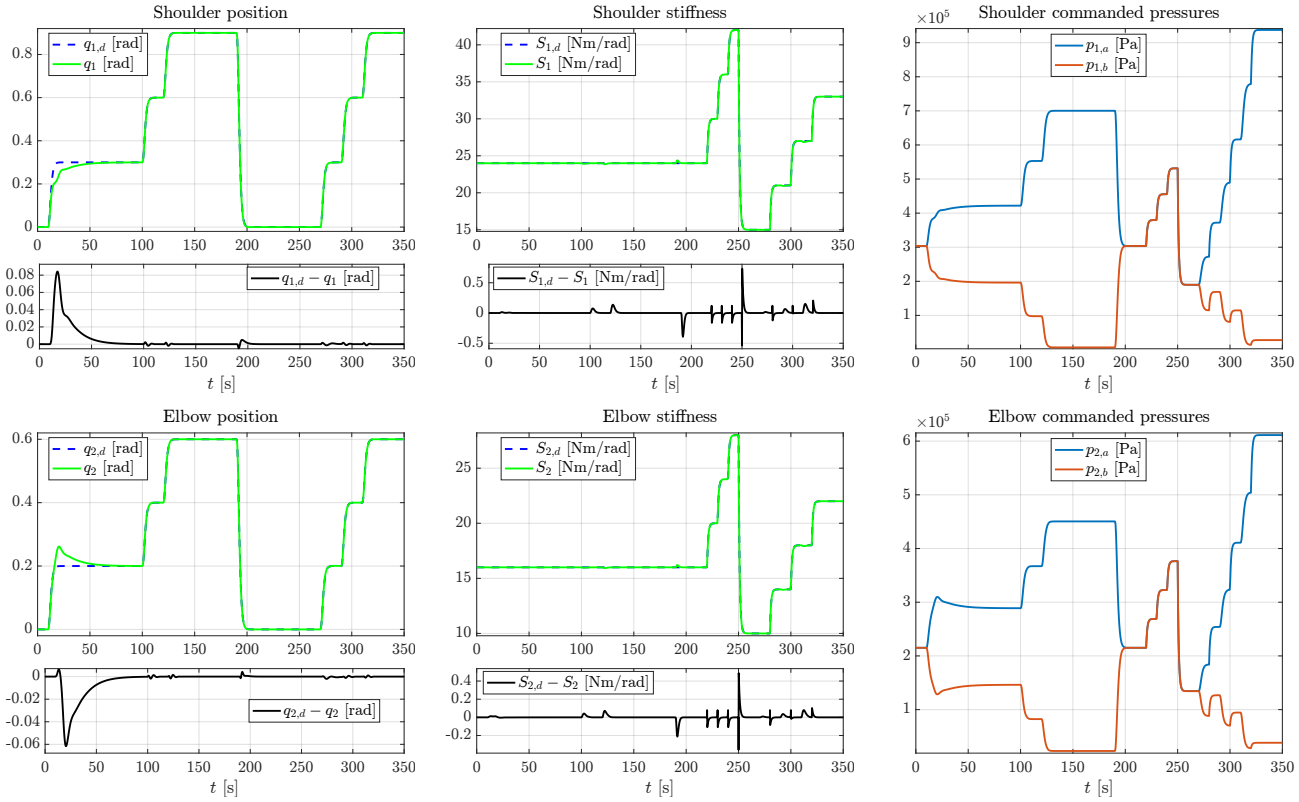

Figure 4. Simulation run of a 2-DoF pneumatic soft robot with initial parameter estimation error of 10% of the real values. Shoulder and elbow references for position and stiffness are specified first alternately (for $t \in [0, 250)$) and then simultaneously (for $t \in [250, 350)$). All commands are asymptotically tracked with feasible pressure commands.

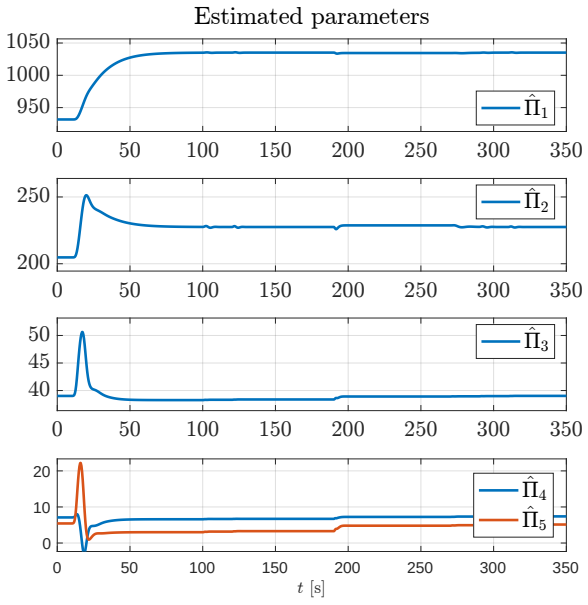

Figure 5. Evolution of the estimated parameter vector for the simulation scenario of Fig. 4. Parameter estimates are rapidly adjusted at the beginning of the simulation and then remain bounded.

larger values of K_π allow achieving faster parameter adaptation response, but, depending on how large is the initial estimation error, attention should be drawn, in order not to drive system to instability during the very first instants.

As for the position tracking error dynamics, the controller constants are chosen as $K_d = 18$ and $\lambda = 15$. It is important to recall from work of Della Santina et al. (2017) that it is preferable to keep their values low so that natural compliance of the robot is sustained, by reducing static feedback impact on the joints' stiffness. The estimated robot's parameters $\hat{\Pi}$ have been chosen to be 10% less than their real values Π.

Furthermore, desired position and stiffness trajectories, q_d and S_d, have been designed, so as to include in the simulation three phases relating to three possible use-cases: 1) stepwise increasing position commands while stiffness is kept constant, 2) stepwise increasing stiffness commands while position is kept constant, 3) simultaneous stepwise commands for position and stiffness. Referring to Fig. 4 and 5, the three phases are for $t \in [0, 190)$, $t \in [190, 250)$, and $t \in [250, 350)$, respectively. Fig. 4 shows that, as soon as a suitable set of values for the estimated parameters is *learnt*, all position and stiffness commands are effectively tracked. Most importantly, it is shown that position commands are followed with almost null influence on the robot's joint stiffness and viceversa, thus proving that the sought decoupling is achieved. Very short transients of the stiffness can occur, only at the instantaneous changes of positions commands, but no steady state error remains. Such transients can be easily avoided by designing smoother reference signals. The figure also reports the corresponding commanded muscle pressures. Fig. 5 shows the adaptation of the components of the estimated parameter vector, which, as it is known, do not converge to the actual values, but remain bounded.

Experimental Validation

This section presents a final validation of the proposed control approach, using a pneumatic soft-robot system, *GioSte* (Fig. 1), which was developed at the University of Pisa by Tonietti and Bicchi (2002).

Hardware and Software Setup. The robotic system consists of an articulated arm with two rotary joints, each driven by a pair of McKibben muscles in antagonistic configuration. All muscles receive pressurized air from a common air compressor source at 8 bars. Inflation and deflation of each muscle is regulated by a dedicated SMC ITV-2050 electro-pneumatic valve, which receives voltage commands in the range of $[0, 6]$ Volts. Such voltage commands are obtained by suitably converting the pressure signals, as shown later, specified by the proposed controller according to Eq. 10. An ad-hoc valve pre-configuration phase has been carried out, in order to prevent valve chattering, by adjusting the pressure response time so as to suit the current application. The angular positions of the rotary joints are measured through two optical and incremental encoders, HEDS 5500 A12, each attached to the shaft of the corresponding joint pulley. The encoders generate 500 counts per revolution, thus allowing to reach a resolution of $1.6 \cdot 10^{-3}$ rad if read in quadrature mode. A National Instruments PCIe6323 acquisition board is used with its screw terminal, so as to collect encoder data and send voltage-based pressure commands to the valves. Real-time control of the system through implementation of the proposed control algorithm has been done, by using Matlab/Simulink 2014a software, which is connected to the NI acquisition card via input-output drivers.

As for this validation, a single-degree-of-freedom version of the GioSte robotic system is first considered, followed by the results of the two-degree-of-freedom setup.

Actuator Model Identification for the one-link GioSte. A preliminary identification phase has been carried out in order to acquire accurate knowledge of the actuator model, as required by the hypotheses of Th. 1. Given the adopted one-link GioSte robot arm, the identification process has aimed at finding the following four mappings: 1) pressure-to-voltage for muscle a, 1) pressure-to-voltage for muscle b, 3) voltage-to-torque, and 4) voltage-to-stiffness.

The first two mappings have been obtained by applying specific voltage commands, covering the entire operation range, to each of the two antagonistic muscles, a and b, and measuring the corresponding achieved pressures, $p_{1,a}$ and $p_{1,b}$. A linear least squares criterium has been used to determine the following second-order polynomial approximation (also depicted in Fig. 6):

$$\begin{aligned} V_{1,a} &= \left(-0.0044\, p_{1,a}^2 + 0.9020\, p_{1,a} - 0.5115\right) \cdot 10^{-5}\,, \\ V_{1,b} &= \left(-0.0008\, p_{1,b}^2 + 0.8862\, p_{1,b} - 0.5157\right) \cdot 10^{-5}\,. \end{aligned} \tag{16}$$

The obtained mappings have been validated with a different set of voltage values and proved to be sufficiently precise, which is also due to the high accuracy of the internal controllers of each electro-valve.

As for the third and fourth mappings, the two muscles have been actuated by suitably varying the input voltages of their valves, and then measuring the finally attained steady-state joint position q_1 when subject to gravity. More precisely,

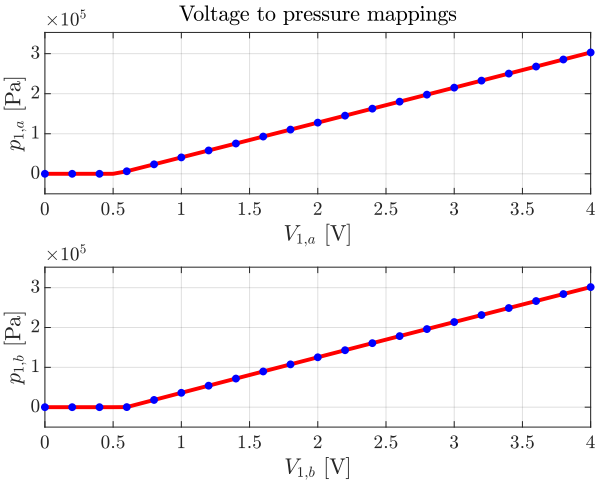

Figure 6. Estimated voltage to pressure mappings for two antagonistic McKibben muscles, actuating the one-link version of the GioSte robot.

experiments consisted of probing the entire voltage to torque and stiffness relation, by applying, *completely in open-loop*, constant voltages to one muscle and varying the one of the other muscle. It is important to state that, during this phase, no form of feedback has been used, so as to measure only the system's stiffness, and not the one induced by a control action. The elastic torque τ_1 has therefore been estimated by exploiting the fact that, when the joint is in the steady state, rotational equilibrium exists and thus, from Eq. 1 and 2, it holds

$$\tau_a - \tau_b - \tau_g = 0\,, \quad \text{with } \tau_g = m_1 g \left(\tfrac{l_1}{2}\right) \sin(q)\,,$$

where τ_a and τ_b are the two torques applied by the two muscles, and τ_g is the gravitational force.

The joint stiffness S, achieved for a given pair of muscle voltages, has been derived by using the model of Eq. 3. By using an analogous least squares fitting algorithm, the following polynomial approximations have been simultaneously found:

$$\begin{aligned} \tau_1 &= \left(6.96 - 2.34\, q_1 - 0.71\, q_1^2\right) V_{1,a} + \\ &\quad -\left(7.03 + 2.07\, q_1 - 0.58\, q_1^2\right) V_{1,b}\,, \\ S_1 &= \left(2.34 - 0.57\, q_1\right) V_{1,a} + \left(2.07 + 0.57\, q_1\right) V_{1,b}\,. \end{aligned} \tag{17}$$

The two mappings provide, for every actual angular position q_1, the torque τ_1 and the stiffness S_1, obtained by applying some specific pair of voltage values, $V_{1,a}$ and $V_{1,b}$.

Finally, the validity of the last mapping, relating the stiffness model, has been experimentally verified, by measuring, for different positions q_1, the change of joint angle Δq_1 induced by a known variation of the gravity force $\Delta\tau_g$, produced by weights at the link tip of the link. Experiments showed that the assumed model is reliable enough for the application. While it is possible to reconstruct more accurate mappings, by using e.g. force sensors mounted on tendons, or even torque sensor mounted on the joint's shaft, it is true that stiffness is a variable that in real applications does not require such high precision. Then, it has been chosen to use the model obtained by Tonietti and Bicchi (2002) for the experiments in this paper.

Experimental Results for the one-link GioSte. To evaluate and show the effectiveness of the proposed decoupling nonlinear adaptive control approach, a set of experiments realizing use-cases similar to the ones considered for the simulation validation have been carried out. Again, the purpose here is to show the ability of the controlled shoulder joint to simultaneously and independently track reference position and stiffness commands. The implemented use-cases are: 1) smoothed stepwise position commands with constant stiffness, 2) smoothed stepwise stiffness commands with constant position, and 3) simultaneous change of position and stiffness. Within all the experiments, the following dynamic model of the one-link GioSte soft-robot has been used:

$$\begin{aligned}\left(I_1 + m_1\left(\tfrac{l_1}{2}\right)\right)\ddot{q}_1 + m_1 g\left(\tfrac{l_1}{2}\right)\sin(q_1) = \\ = K_1\left(\phi_{1,a}(q_1), -\phi_{1,b}(q_1)\right)\begin{pmatrix} p_{1,a} \\ p_{1,b}\end{pmatrix},\end{aligned}$$

$$\begin{aligned}\dot{S}_1 &= -K_1\left(\dot{\phi}_{q,1,a}(q_1), -\dot{\phi}_{q,1,a}(q_1)\right)\begin{pmatrix} p_{1,a} \\ p_{1,b}\end{pmatrix} + \\ &+ -K_1\left(\phi_{q,1,a}(q_1), -\phi_{q,1,a}(q_1)\right)\begin{pmatrix} \dot{p}_{1,a} \\ \dot{p}_{1,b}\end{pmatrix},\end{aligned}$$

where the viscous friction term has been neglected. Then, the regressor matrix from Theorem 1 is

$$Y_* = \left(\ddot{q}_{1,r}, \sin(q_1)\right),$$

and the unknown parameter vector is

$$\Pi = (\Pi_1, \Pi_2)^T = \left(\left(I_1 + m_1\left(\tfrac{l_1}{2}\right)^2\right)/K_1, m_1 g\left(\tfrac{l_1}{2}\right)/K_1\right)^T.$$

Moreover, before proceeding to presenting the experimental results, referring to Remark 3, we can show that the numerical time differentiation of the term $\Phi^\dagger(q_1)\tau_*$, involved in Eq. 8 of Th. 1 can be avoided by applying the chain rule. Indeed it holds:

$$\frac{d}{dt}\left(\Phi^\dagger(q_1)\,\tau_*\right) = \Phi^\dagger_q(q_1)\,\dot{q}_1\,\tau_* + \Phi^\dagger(q_1)\frac{\partial \tau_*}{\partial q_1}\dot{q}_1,$$

where

$$\begin{aligned}\frac{\partial \tau_*}{\partial q_1} &= \frac{\partial}{\partial q_1}\left(Y_*(q_1, \dot{q}_1, \dot{q}_{1,r}, \ddot{q}_{1,r})\,\hat{\Pi} + K_d\,\sigma\right) = \\ &= \frac{\partial}{\partial q_1}\left(\left(\ddot{q}_{1,r}, \sin(q_1)\right)(\hat{\Pi}_1, \hat{\Pi}_2)^T\right) + \\ &+ \frac{\partial}{\partial q_1}\left(K_d\left(\dot{q}_{1,d} - \dot{q}_1 + \Lambda\left(q_{1,d} - q_1\right)\right)\right) = \\ &= \cos(q_1)\,\hat{\Pi}_2 - K_d\Lambda,\end{aligned}$$

which shows that no information regarding the acceleration $\ddot{q}_1$ is in fact necessary. As it is known, this fact allows avoiding noise amplification effects that would occur in numerical differentiation.

Moving now on to the experiments, we have chosen desired position and stiffness values that are compliant with our hardware. Some of the factors playing a role in such choice are the nominal and minimal muscle lengths and the maximal muscle pressure (cf. also by Medrano-Cerda et al. (1995)). We have carried out three tests where the following gain values of the adaptive and decoupling controller have been chosen: $K_d = 2$, $\Lambda = 10$, and $K_\pi = 45$. Despite the slower tracking error obtained, such values have been chosen in order to be able to present some important features in the following plots.

During the first experiment, whose results are presented in Fig. 7, a stepwise reference signal $q_{1,d}(t)$ for the joint position, ranging from 0 to 0.3 radians, is given, with a constant desired stiffness $S_d(t) = 10$ Nm/rad. The figure shows that, despite an initial tracking delay, mostly due to the imprecise value of the parameters, all position commands are asymptotically followed, while stiffness is maintained practically constant. The controlled system is able to cope with both the uncertainties of the left hand side of the model, and with the one of the construction-dependent constant K_1 of the pneumatic actuator. Moreover it also recovers from the residual error of the identification process, due to an inevitably not exact estimation of the nominal and minimum lengths of the two muscles. Another important feature to observe is how the controller's internal state ν evolves, nicely adjusting its value, in order to assure the sought decoupling. The commanded voltages $V_{1,a}$ and $V_{1,b}$ remain always within the feasible range. It can also be observed that the amplitude of the steady-state tracking error is of the same order of encoder resolution, and thus it could be reduced through the use of encoders with more pulses per revolution.

As a complementary second experiment, shown in Fig. 8, the desired stiffness is changed stepwise from 7 to 10 Nm/rad, while the desired position is kept constant at 0.2 rad. Similarly to the previous experiment, the largest tracking error of both stiffness and position occurs during an initial phase, when the adaptive control is still trying to *learn* a suitable combination of parameter values.

The last of the three experiments combines the two previous scenarios, including commanded position and stiffness signals that change simultaneously. It can be seen from Fig. 9 that the adaptive and decoupling controller allows tracking such references, with practically no interference with each other. As shown by De Luca and Lucibello (1998), dynamic feedback linearization is able to achieve perfect decoupling, in the absence of measurement noise and model uncertainties. As said in the introduction, leveraging on the idea therein proposed of introducing a stiffness dynamics has allowed us to derive our present adaptive approach, which has shown to be an effective solution.

Comparison Between Open- and Closed-loop Adaptive Stiffness Control. Let us now proceed to further analyze the performance of the proposed control approach, by showing the different behavior of the adaptive open-loop control algorithm described in Tonietti and Bicchi (2002) and the above proposed closed-loop stiffness control.

To this purpose, a first set of experiments has been designed in order to investigate how the two systems respond to stepwise position commands with different rise times T_r, while the desired stiffness remains constant, i.e. $S_d = \bar{S}_d$. The comparison has been done by choosing the controller gain values $K_d = 12$, $\Lambda = 1.8$, and $K_\pi = 45$. First, Fig. 10 reports the behavior of the controlled GioSte robot with desired position rise time set to $T_r = 6.7158$ seconds. Smoothed position reference steps are applied at

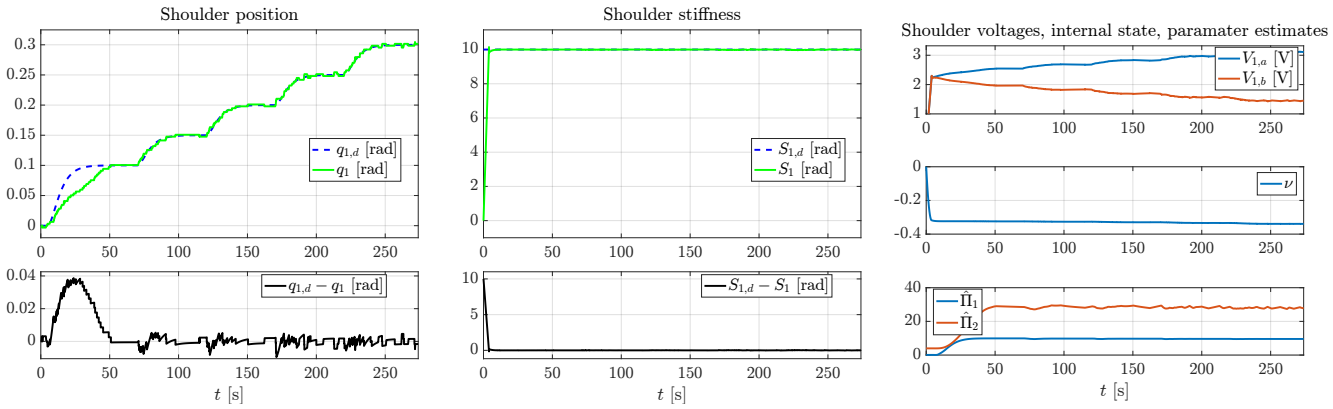

Figure 7. Experiment #1 - Smoothed stepwise position commands with constant stiffness. The position tracking error gradually decays as parameter adaptation advances. After adaptation, the tracking error is mostly affected by the noise of pressure regulators and has the same order of amplitude of the encoder resolution. The impact of position changes on the joint stiffness is negligible as desired. Estimated parameters, internal control state, and commanded voltages are bounded and smooth.

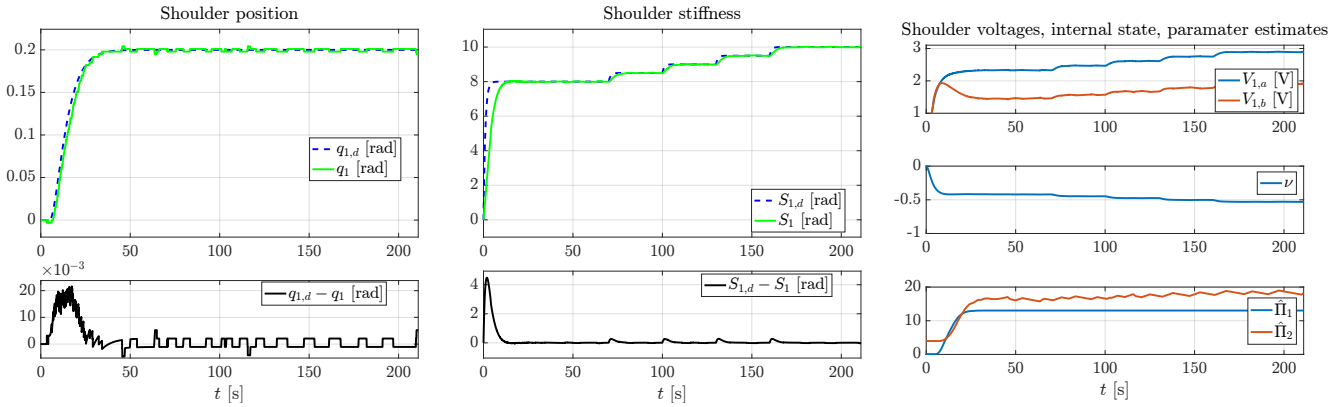

Figure 8. Experiment #2 - Smoothed stepwise stiffness commands with constant position. Dually to the previous experiment, the stiffness tracking error asymptotically converges. The position tracking error is not affected by the stiffness commands. Estimated parameters, internal control state and commanded voltages are bounded and smooth.

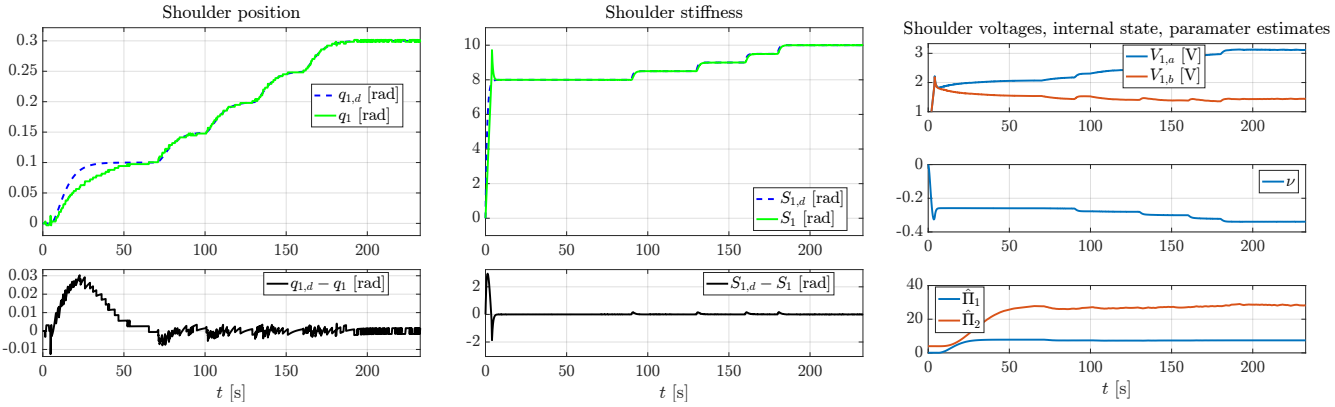

Figure 9. Experiment #3 - Simultaneous position and stiffness commands. All references are successfully tracked with no apparent mutual interference as desired.

$t = 0$ and $t = 36$ seconds. It can be observed that, during the initial interval, the open-loop approach is able to faster track the desired position command; in fact, the requirement to adapt also to the stiffness dynamics provides the algorithm with some more conservative and slower behavior. After this first adaptation phase, the closed-loop approach has a similar response time as the open-loop one, as for what it concerns the position, but with the additional advantage that a smoother position tracking is achieved; however, due to the imposed stiffness dynamics, one can notice a transient in the stiffness tracking. It can also be seen that estimated parameters, the commanded voltages, and the internal control state ν well-behave from a numerical standpoint and remain bounded.

Furthermore, Fig. 11 summarizes the two approaches for three decreasing position rise times, namely $T_r = 4.39$, $T_r =$

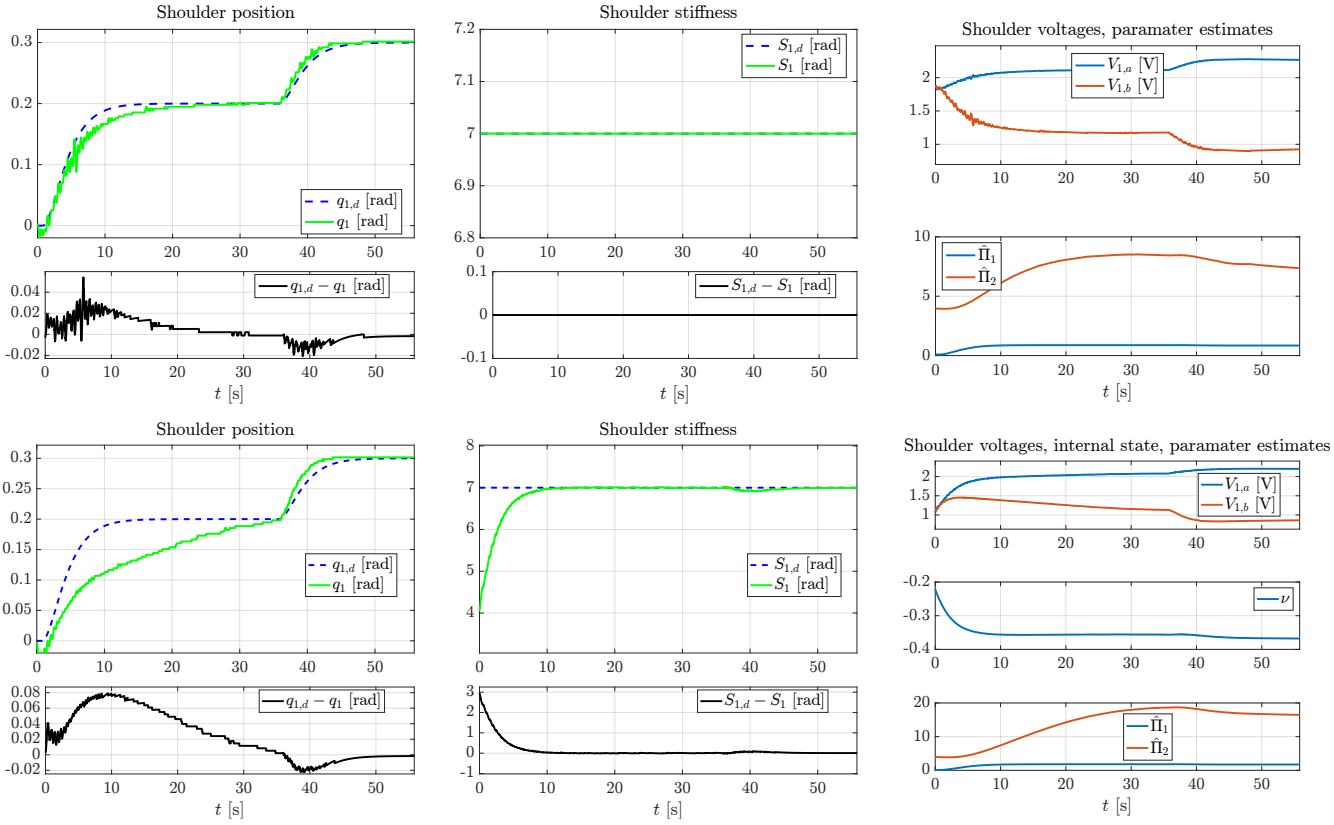

Figure 10. Experiment #4 - Comparison of the adaptive open-loop (first row) and closed-loop (second row) stiffness control with position references with rise time $T_r = 6.7158$ seconds. During the first interval, for $t < 40$ seconds, the open-loop approach is able to track faster the desired position command; indeed, the requirement to adapt also to the stiffness dynamics provides the algorithm with some more conservative and slower behavior, leading to the observed initial lag in the closed-loop response. After this first adaptation phase, the closed-loop approach has a similar response time as the open-loop one, as for what it concerns the position, but with the additional advantage that a smoother position tracking is achieved; however, due to the imposed stiffness dynamics, one can notice a transient in the stiffness tracking.

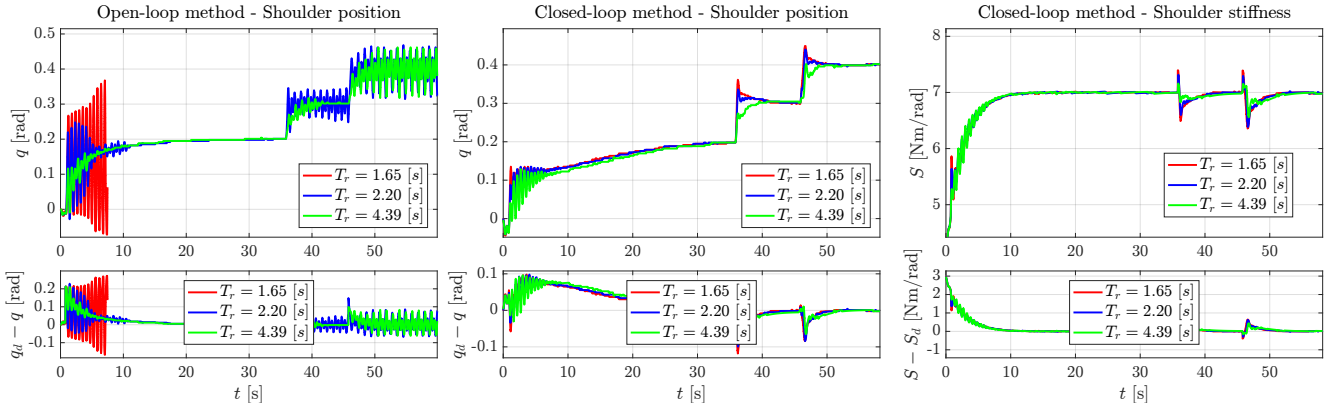

Figure 11. Experiment #5 - Comparison of open-loop (leftmost) and closed-loop (middle and rightmost) stiffness control for position references with decreasing rise times. Smoothed position reference steps are applied at $t = 0$, $t = 36$, and 46 seconds. While the open-loop solution starts to experience an oscillatory behavior, more apparent as T_r decreases, and eventually goes to instability, the closed-loop one, after some initial oscillations, is capable of preserving the system's stability.

2.20 and $T_r = 1.65$ seconds. Smoothed position reference steps are applied at $t = 0$, $t = 36$, and 46 seconds; they are not reported in the figures for the sake of clarity. The stiffness in open-loop is constantly maintained to 7 Nm/rad as in the previous experiment of Fig. 10. The leftmost plot of the figure shows that the system controlled via the open-loop stiffness method starts to experience an oscillatory behavior, more apparent as T_r decreases, and eventually goes to instability. The two other plots of the figure, the middle and rightmost, shows that, with the same setup, after some initial oscillations, the closed-loop stiffness control can preserve the system's stability. Indeed, the residual inaccuracy in the actuator model identification process may lead to such an oscillatory evolution, while the introduction of stiffness dynamics has the further benefit of providing the resulting system additional inertia. It is, thus, the faster rise time

request in the position command $q_d(t)$ mostly responsible for the increase of the oscillatory and finally unstable behavior of the system controlled via the open-loop stiffness approach.

Proceeding to a second type of experiments, we have investigated the effect of stepwise stiffness commands on the joint position. To this aim, the desired position is kept constant and the stiffness reference is stepwise changing. Fig. 12 reveals that both controlled systems remain stable, but the impact of stiffness reference change on the position is larger in the case of the open-loop solution, which ultimately also show how our approach can embed the controlled system with better capacity of stiffness to position decoupling.

Broadly speaking, the fundamental difference between these two approaches lays in the general principles of open and closed-loop control frameworks. The advantage of stiffness regulation has been foreseen by Medrano-Cerda et al. (1995) and the vision of model-based independent joint position and stiffness control of electrically driven VSAs has been theoretically proposed by Palli et al. (2007) and Palli et al. (2008). The closure of stiffness loop is supposed to lead to the better performance when the desired reference profile of stiffness is time varying. Indeed, the inclusion of dynamics (i.e. an integrator) in the stiffness control allows the closed-loop system to better cope with the non-modeled dynamics of the mechanical system. On the other side, the implementation of the open-loop control by Tonietti and Bicchi (2002) is easier, which finally drives to the conclusion that specific use-cases will determine the choice of proper control approach.

Experimental Validation for the two-link GioSte. This subsection presents results of the validation and performance evaluation of the proposed control law the full two degree-of-freedom robot arm of Fig. 1. In this setup, the first link q_1 will act as the robot's *shoulder* and the second one q_2 will represent its *elbow*. Similarly to the procedure previously described for the one-DoF robot, we have carried out an identification process for the two-link GioSte leading to the following mappings:

$$\begin{aligned}
\tau_1 &= \left(2.28 - 2.87\,q_1 + 2.16\,q_1^2\right)\,V_{1,a} + \\
&\quad -(2.54 + 2.28\,q_1 + 6.09\,q_1^2)\,V_{1,b}\,, \\
\tau_2 &= \left(6.96 - 2.34\,q_2 - 0.71\,q_2^2\right)\,V_{2,a} + \\
&\quad -(7.03 + 2.07\,q_2 - 0.58\,q_2^2)\,V_{2,b}\,, \\
S_1 &= (2.87 + 0.83\,q_1)\;V_{1,a} + (2.28 - 0.83\,q_1)\;V_{1,b}\,, \\
S_2 &= (2.34 - 0.57\,q_2)\;V_{2,a} + (2.07 + 0.57\,q_2)\;V_{2,b}\,.
\end{aligned}$$

The same mapping as in Eq. 16 has been used for the second link to relate the pressure $p_{2,a}$ and $p_{2,b}$ with the voltages $V_{2,a}$ and $V_{2,b}$. Moreover, the controller's gains are $K_d = \mathrm{diag}(K_{1,d}, K_{2,d}) = \mathrm{diag}(15, 2)$, $\Lambda = \mathrm{diag}(\Lambda_1, \Lambda_2) = \mathrm{diag}(8, 8)$, and $K_\pi = 45\,I_{5\times5}$.

Before moving to the experiments, it is worthwhile to observe, referring to Remark 3, that the Jacobian matrix

$$\frac{\partial \tau_*}{\partial q} = \left\{ \frac{\partial \tau_{*,i}}{\partial q_j} \right\}\,,\ \mathrm{i,j}\ \in \{1,2\}\,,$$

includes the following terms:

$$\begin{aligned}
\frac{\partial \tau_{*,1}}{\partial q_1} &= \frac{\partial}{\partial q_1}\left(Y_{*,1}(\cdot)\,\hat{\Pi} + K_{1,d}\,\sigma_1\right) = \\
&= \frac{\partial}{\partial q_1}\left((\ddot{q}_{1,r}, \ddot{q}_{2,r}, Y_{13}(\cdot), s_1, s_{12})\,\hat{\Pi}\right) + \\
&+ \frac{\partial}{\partial q_1}\left(K_{1,d}\left(\dot{q}_{1,d} - \dot{q}_1 + \Lambda_1\left(q_{1,d} - q_1\right)\right)\right) = \\
&= \Lambda_1\,s_2\,\dot{q}_2\,\hat{\Pi}_3 + c_1\hat{\Pi}_4 + c_{12}\hat{\Pi}_5 - K_{1,d}\Lambda_1\,, \\
\\
\frac{\partial \tau_{*,1}}{\partial q_2} &= \frac{\partial}{\partial q_2}\left(Y_{*,1}(\cdot)\,\hat{\Pi} + K_{1,d}\,\sigma_1\right) = \\
&= -\left(\left(2\ddot{q}_{1,r} + \ddot{q}_{2,r} + \tfrac{1}{2}\Lambda_2\dot{q}_2\right)\,s_2 + \right. \\
&\quad \left. + \left(\dot{q}_1 + \tfrac{1}{2}\dot{q}_2 + \dot{q}_{1,r} + \tfrac{1}{2}\dot{q}_{2,r}\right)\,\dot{q}_2 c_2\right)\,\hat{\Pi}_3 + c_{12}\,\hat{\Pi}_5\,, \\
\\
\frac{\partial \tau_{*,2}}{\partial q_1} &= \frac{\partial}{\partial q_1}\left(Y_{*,2}(\cdot)\hat{\Pi} + K_{2,d}\,\sigma_2\right) = \\
&= \frac{\partial}{\partial q_1}\left((0, \ddot{q}_{1,r} + \ddot{q}_{2,r}, Y_{23}(\cdot), 0, s_{12})\,\hat{\Pi}\right) + \\
&+ \frac{\partial}{\partial q_1}\left(K_{2,d}\left(\dot{q}_{2,d} - \dot{q}_2\right) + \Lambda_2\left(q_{2,d} - q_2\right)\right) = \\
&= \tfrac{1}{2}\Lambda_1\dot{q}_2\,s_2\,\hat{\Pi}_3 + c_{12}\,\hat{\Pi}_5\,, \\
\\
\frac{\partial \tau_{*,2}}{\partial q_2} &= \left(\left(\dot{q}_1^2 + \tfrac{1}{2}\dot{q}_1\dot{q}_2 - \tfrac{1}{2}\dot{q}_{1,r}\dot{q}_2\right)\,c_2 - \ddot{q}_{1,r}\,s_2\right)\,\hat{\Pi}_3 + \\
&+ c_{12}\,\hat{\Pi}_5 - K_{2,d}\,\Lambda_2\,.
\end{aligned}$$

Accordingly, no joint acceleration and jerk are also needed for the two-DoF case.

The shoulder joint is commanded to simultaneously follow smoothed stepwise trajectories ranging from 0 to 0.25 radians for the positions, and 17 to 19 Nm/rad for the stiffness; the elbow joint is required to track smoothed stepwise trajectories ranging from 0 to 0.15 radians for the positions, and 12 to 14 Nm/rad for the stiffness. The obtained results in Fig. 13 show that independent and simultaneous tracking capabilities for both position and stiffness desired evolution are achieved, while the estimated parameters converge as depicted in Fig. 14. As anticipated, the largest tracking error is observed during the adaptation phase, which is due to the parameter uncertainty, and during the position transients, caused by the residual coupling between joints. The change of stiffness reference has a negligible impact on the position. Thus, the effectiveness of proposed method has been confirmed also for multi-DoF setups.

Conclusion

In this article a novel approach for adaptive and decoupling control of position and stiffness in pneumatic soft-robots has been presented. The approach achieves the desired decoupling by using the control degree of freedom, laying in the kernel of known part of the actuator matrix, plus an additional dynamic compensation that is made available by the introduction of the stiffness dynamics. The approach has been validated first via simulations and through experiments with a two-degree-of-freedom robot soft robot. Validation has shown that joint position and stiffness are effectively tracked in different use-cases. A formal proof of the stability of the tracking error for the approach has also been provided.

The solution has shown to have several advantages. First, it is robust to model uncertainties and, if stiffness

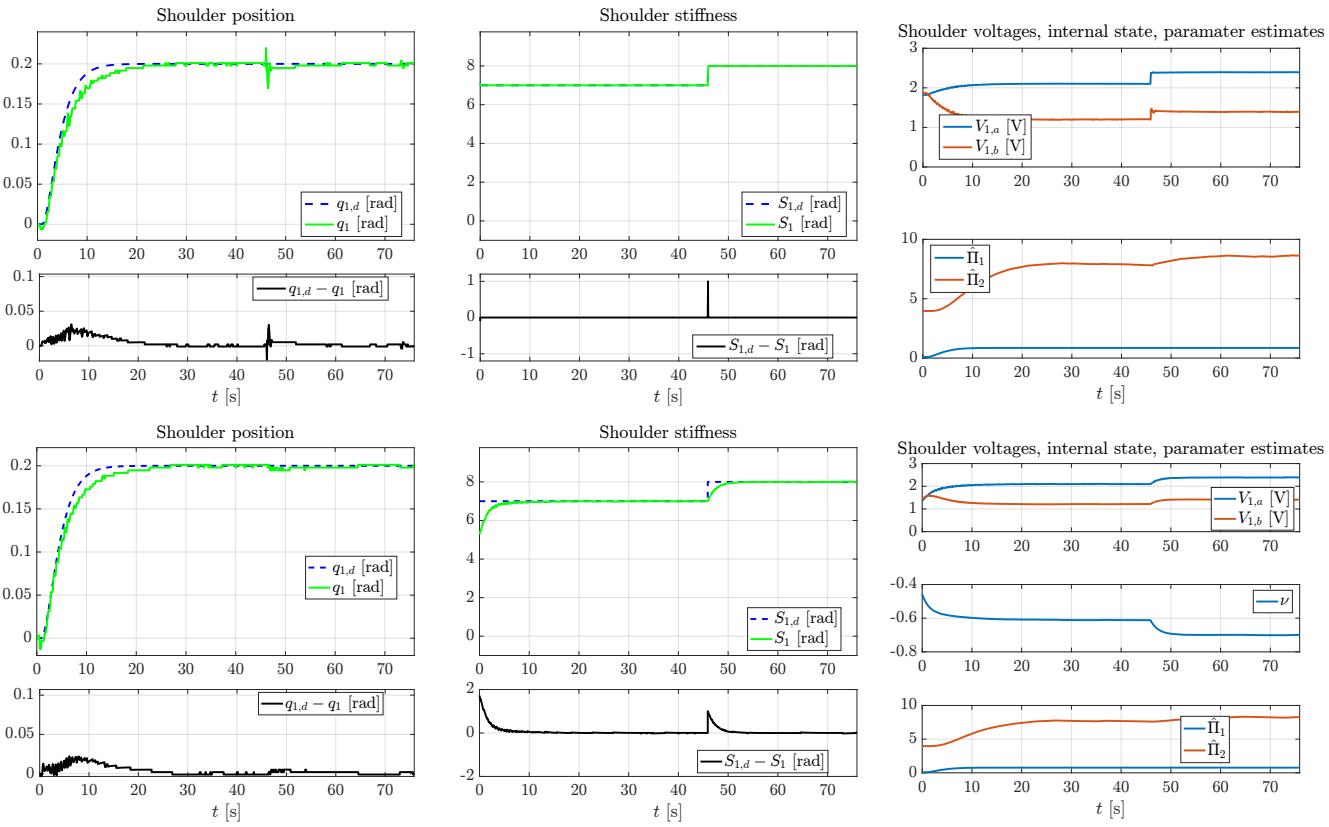

Figure 12. Experiment #6 - Adaptive open-loop (first row) and closed-loop (second row) control of stiffness for stepwise stiffness reference. The controlled system under open-loop stiffness regulation experiences position disturbance during the transient of stiffness reference. On the contrary, the closed-loop control of stiffness can suppress the oscillation of joint position.

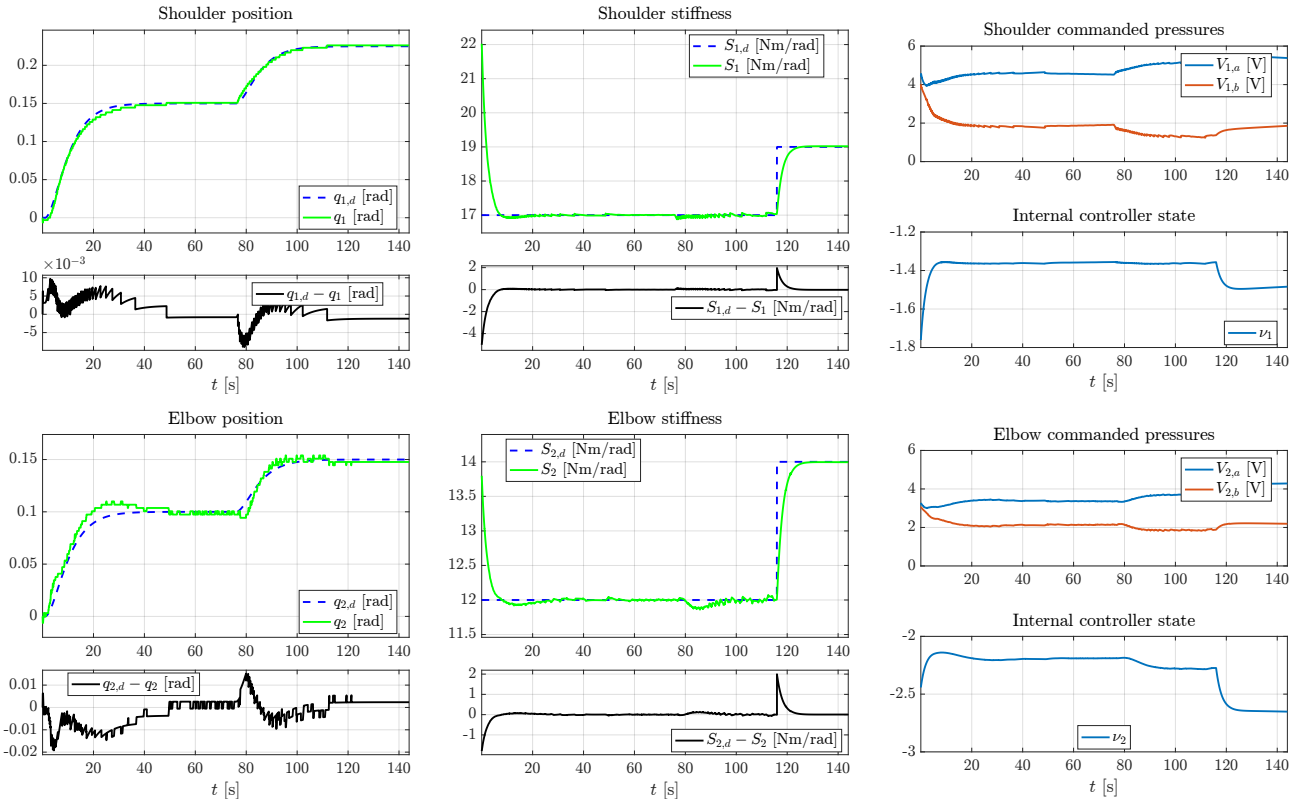

Figure 13. Experiment #7 - Experimental run of a 2-DoF pneumatic soft robot with smoothed stepwise references for position and stiffness of shoulder and elbow. Tracking errors converge to zero and there is no significant mutual impact between position and stiffness control. During the transients, a small position tracking error is induced due to the residual coupling between the joints.

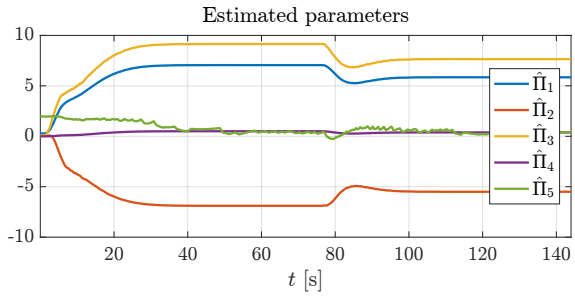

Figure 14. Evolution of the estimated parameter vector for the experiment shown in Fig. 13. Parameter estimates are adjusted at the beginning of the experiment and then remain bounded.

reference is constant or slowly-varying, also to actuator uncertainties. Secondly, it requires computation of only the first time derivative of stiffness and of the second time derivative of position. No further differentiation is needed, thus simplifying practical implementations. Third, it allows joint stiffness to be controlled in closed loop, thereby making the system more capable of following various position trajectory profiles, as shown in experiments. Practically, this means that joints can achieve faster movements (even with lower stiffness) when compared to the open-loop case, hence potentially improving the safety of soft robots when used for human-robot interaction.

The main limitation of the current approach stems in the assumption that part of the actuator model is known, which has required us to perform an initial identification phase. However, we believe that the approach can be generalized for fully unknown actuator matrices, as well as for different classes of pneumatically and electrically driven soft robots. This objective can be achieved e.g. by using force or torque sensors, which would allow better estimation of the stiffness and thus more effective closed-loop control. A second limitation of the current hardware is related to the present mechanical coupling among joint pulleys, shafts, and muscles, which is unable to effectively support fast motions without experiencing slippage and inducing measurement errors. Albeit slower experiments have been shown, we are confident that better results can be achieved with a future hardware upgrade by adopting better mechanical solutions for such connections and using more consistent materials for the artificial muscles. With the same objective of achieving faster motions, but with a different type of actuators, some seminal work has already been initiated by Lukic et al. (2019), with an electric antagonistic VSA setup characterized by more reliable mechanical structures and faster natural dynamics.

It is also worth saying that the scalability of the proposed method, and in fact that of other adaptive control approaches, relies on the derivation of the regressor form of a robot's dynamics. To this respect, very recently, novel approaches, such as that by Marcucci et al. (2017), have introduced automatic generation methods, aiming at reducing the amount of information needed to model and control a robot manipulator, and thus also potentially improving the efficiency of the proposed solution.

A final closing comment is connected to the observation by Albu-Schaeffer and Bicchi (2016) that a lot of work has still to be done in the field of impedance estimators, as well as with they usage with VSA mechanisms. We believe that the development of closed-loop control approaches, such as ours, will encourage the establishment of theoretical and technical framework for stiffness estimation and exploitation in advanced soft robotic systems.

Funding

The research leading to these results has been partially funded by the Ministry of Education, Science and Technological Development of the Republic of Serbia, under the National contract TR-35003.

Acknowledgements

The authors would like to thank Prof. Antonio Bicchi for his insightful suggestions, and Eng. Franco Angelini and Eng. Riccardo Mengacci for helpful discussions on many experimental issues.

References

Ajoudani A, Zanchettin AM, Ivaldi S, Albu-Schäffer A, Kosuge K and Khatib O (2018) Progress and prospects of the human–robot collaboration. *Autonomous Robots* : 1–19.

Albu-Schaeffer A and Bicchi A (2016) *Actuators for Soft Robotics*, chapter 21. Springer Handbook of Robotics, pp. 499–530.

Albu-Schäffer A, Haddadin S, Ott C, Stemmer A, Wimböck T and Hirzinger G (2007) The dlr lightweight robot: design and control concepts for robots in human environments. *Industrial Robot: an international journal* 34(5): 376–385.

Albu-Schaffer A and Hirzinger G (2002) Cartesian impedance control techniques for torque controlled light-weight robots. In: *Robotics and Automation, 2002. Proceedings. ICRA'02. IEEE International Conference on*, volume 1. IEEE, pp. 657–663.

Angelini F, Della Santina C, Garabini M, Bianchi M, Gasparri GM, Grioli G, Catalano MG and Bicchi A (2018) Decentralized trajectory tracking control for soft robots interacting with the environment. *IEEE Transactions on Robotics* .

Best CM, Gillespie MT, Hyatt P, Rupert L, Sherrod V and Killpack MD (2016) A new soft robot control method: Using model predictive control for a pneumatically actuated humanoid. *IEEE Robotics & Automation Magazine* 23(3): 75–84.

Bicchi A and Tonietti G (2002) Design, realization and control of soft robot arms for intrinsically safe interaction with humans. In: *Proc. IARP/RAS Workshop on Technical Challenges for Dependable Robots in Human Environments*. pp. 79–87.

Bicchi A and Tonietti G (2004) Fast and" soft-arm" tactics [robot arm design]. *IEEE Robotics & Automation Magazine* 11(2): 22–33.

Caldwell DG, Medrano-Cerda GA and Goodwin M (1995) Control of pneumatic muscle actuators. *IEEE control systems* 15(1): 40–48.

Cherubini A, Passama R, Crosnier A, Lasnier A and Fraisse P (2016) Collaborative manufacturing with physical human–robot interaction. *Robotics and Computer-Integrated Manufacturing* 40: 1–13.

Chou CP and Hannaford B (1996) Measurement and modeling of mckibben pneumatic artificial muscles. *IEEE Transactions on robotics and automation* 12(1): 90–102.

Colbrunn RW, Nelson GM and Quinn RD (2001) Design and control of a robotic leg with braided pneumatic actuators. In: *Proceedings 2001 IEEE/RSJ International Conference on Intelligent Robots and Systems. Expanding the Societal Role of*

Robotics in the the Next Millennium (Cat. No. 01CH37180), volume 2. IEEE, pp. 992–998.

De Luca A, Flacco F, Bicchi A and Schiavi R (2009) Nonlinear decoupled motion-stiffness control and collision detection/reaction for the vsa-ii variable stiffness device. In: *2009 IEEE/RSJ International Conference on Intelligent Robots and Systems*. IEEE, pp. 5487–5494.

De Luca A and Lucibello P (1998) A general algorithm for dynamic feedback linearization of robots with elastic joints. In: *Robotics and Automation, 1998. Proceedings. 1998 IEEE International Conference on*, volume 1. IEEE, pp. 504–510.

Della Santina C, Bianchi M, Grioli G, Angelini F, Catalano M, Garabini M and Bicchi A (2017) Controlling soft robots: balancing feedback and feedforward elements. *IEEE Robotics & Automation Magazine* 24(3): 75–83.

Dietrich A, Ott C and Albu-Schäffer A (2015) An overview of null space projections for redundant, torque-controlled robots. *The International Journal of Robotics Research* 34(11): 1385–1400.

Garabini M, Passaglia A, Belo F, Salaris P and Bicchi A (2011) Optimality principles in variable stiffness control: The vsa hammer. In: *Intelligent Robots and Systems (IROS), 2011 IEEE/RSJ International Conference on*. IEEE, pp. 3770–3775.

Gavrilović M and Marić M (1969) Positional servo-mechanism activated by artificial muscles. *Medical and Biological Engineering* 7(1): 77–82.

Grioli G and Bicchi A (2010) A non-invasive real-time method for measuring variable stiffness. In: *Robotics Science and Systems VI*. pp. 90–96.

Grioli G, Wolf S, Garabini M, Catalano M, Burdet E, Caldwell D, Carloni R, Friedl W, Grebenstein M, Laffranchi M, Lefeber D, Stramigioli S, Tsagarakis N, Van Damme M, Vanderborght B, Albu-Schäffer A and Bicchi A (2015) Variable stiffness actuators: The user's point of view. *The International Journal of Robotics Research* 34(6): 727–743.

Haddadin S, Albu-Schäffer A and Hirzinger G (2009) Requirements for safe robots: Measurements, analysis and new insights. *The International Journal of Robotics Research* 28(11-12): 1507–1527.

Hogan N (1985) Impedance control: An approach to manipulation: Part ii—implementation. *Journal of dynamic systems, measurement, and control* 107(1): 8–16.

Keppler M, Lakatos D, Ott C and Albu-Schäffer A (2016) A passivity-based approach for trajectory tracking and link-side damping of compliantly actuated robots. In: *Robotics and Automation (ICRA), 2016 IEEE International Conference on*. IEEE, pp. 1079–1086.

Keppler M, Lakatos D, Ott C and Albu-Schäffer A (2018) Elastic structure preserving (esp) control for compliantly actuated robots. *IEEE Transactions on Robotics* 34(2): 317–335.

Khatib O (1987) A unified approach for motion and force control of robot manipulators: The operational space formulation. *IEEE Journal on Robotics and Automation* 3(1): 43–53.

Lukic B, Jovanovic K and Sekara T (2019) Cascade control of antagonistic vsa-an engineering control approach to a bio-inspired robot actuator. *Frontiers in neurorobotics* 13: 69.

Lukić BZ, Jovanović KM and Kvaščev GS (2016) Feedforward neural network for controlling qbmove maker pro variable stiffness actuator. In: *Neural Networks and Applications (NEUREL), 2016 13th Symposium on*. IEEE, pp. 1–4.

Marcucci T, Della Santina C, Gabiccini M and Bicchi A (2017) Towards minimum-information adaptive controllers for robot manipulators. In: *2017 American Control Conference (ACC)*. IEEE, pp. 4209–4214.

Medrano-Cerda GA, Bowler CJ and Caldwell DG (1995) Adaptive position control of antagonistic pneumatic muscle actuators. In: *Proceedings 1995 IEEE/RSJ International Conference on Intelligent Robots and Systems. Human Robot Interaction and Cooperative Robots*, volume 1. IEEE, pp. 378–383.

Migliore SA, Brown EA and DeWeerth SP (2007) Novel nonlinear elastic actuators for passively controlling robotic joint compliance. *Journal of Mechanical Design* 129(4): 406–412.

Niiyama R, Nagakubo A and Kuniyoshi Y (2007) Mowgli: A bipedal jumping and landing robot with an artificial musculoskeletal system. In: *Robotics and Automation, 2007 IEEE International Conference on*. IEEE, pp. 2546–2551.

Ott C, Albu-Schaffer A, Kugi A and Hirzinger G (2008) On the passivity-based impedance control of flexible joint robots. *IEEE Transactions on Robotics* 24(2): 416–429.

Palli G, Melchiorri C and De Luca A (2008) On the feedback linearization of robots with variable joint stiffness. In: *Robotics and Automation, 2008. ICRA 2008. IEEE International Conference on*. IEEE, pp. 1753–1759.

Palli G, Melchiorri C, Wimbock T, Grebenstein M and Hirzinger G (2007) Feedback linearization and simultaneous stiffness-position control of robots with antagonistic actuated joints. In: *Robotics and Automation, 2007 IEEE International Conference on*. IEEE, pp. 4367–4372.

Petit F, Daasch A and Albu-Schäffer A (2015) Backstepping control of variable stiffness robots. *IEEE Transactions on Control Systems Technology* 23(6): 2195–2202.

Piazza C, Catalano MG, Godfrey SB, Rossi M, Grioli G, Bianchi M, Zhao K and Bicchi A (2017) The softhand pro-h: a hybrid body-controlled, electrically powered hand prosthesis for daily living and working. *IEEE Robotics & Automation Magazine* 24(4): 87–101.

Potkonjak V, Svetozarevic B, Jovanovic K and Holland O (2011) The puller-follower control of compliant and noncompliant antagonistic tendon drives in robotic systems. *International Journal of Advanced Robotic Systems* 8(5): 143–155.

Semini C, Tsagarakis NG, Guglielmino E, Focchi M, Cannella F and Caldwell DG (2011) Design of hyq–a hydraulically and electrically actuated quadruped robot. *Proceedings of the Institution of Mechanical Engineers, Part I: Journal of Systems and Control Engineering* 225(6): 831–849.

Seok S, Wang A, Chuah MYM, Hyun DJ, Lee J, Otten DM, Lang JH and Kim S (2015) Design principles for energy-efficient legged locomotion and implementation on the mit cheetah robot. *IEEE/ASME Transactions on Mechatronics* 20(3): 1117–1129.

Siciliano B and Khatib O (2008) *Springer handbook of robotics*. Springer Science & Business Media.

Slotine JJE and Li W (1987) On the adaptive control of robot manipulators. *The International Journal of Robotics Research* 6(3): 49–59.

Slotine JJE and Li W (1991) *Applied nonlinear control*. Englewood Cliffs, NJ, 07632: Prentice hall.

Spong MW (1989) Adaptive control of flexible joint manipulators. *Systems & Control Letters* 13(1): 15–21.

Tonietti G and Bicchi A (2002) Adaptive simultaneous position and stiffness control for a soft robot arm. *IEEE/RSJ International Conference on Intelligent Robots and Systems* 2: 1992–1997.

Van Ham R, Sugar TG, Vanderborght B, Hollander KW and Lefeber D (2009) Compliant actuator designs. *IEEE Robotics & Automation Magazine* 16(3).

Vanderborght B, Albu-Schäffer A, Bicchi A, Burdet E, Caldwell DG, Carloni R, Catalano M, Eiberger O, Friedl W, Ganesh G, Garabini M, Grebenstein M, Grioli G, Haddadin S, Hoppner H, Jafari A, Laffranchi M, Lefeber D, Petit F, Stramigioli S, Tsagarakis N, Van Damme M, Van Ham R, Visser L and Wolf S (2013) Variable impedance actuators: A review. *Robotics and autonomous systems* 61(12): 1601–1614.

Vanderborght B, Van Ham R, Verrelst B, Van Damme M and Lefeber D (2008) Overview of the lucy project: Dynamic stabilization of a biped powered by pneumatic artificial muscles. *Advanced Robotics* 22(10): 1027–1051.

Verrelst B, Van Ham R, Vanderborght B, Daerden F, Lefeber D and Vermeulen J (2005) The pneumatic biped “lucy” actuated with pleated pneumatic artificial muscles. *Autonomous Robots* 18(2): 201–213.